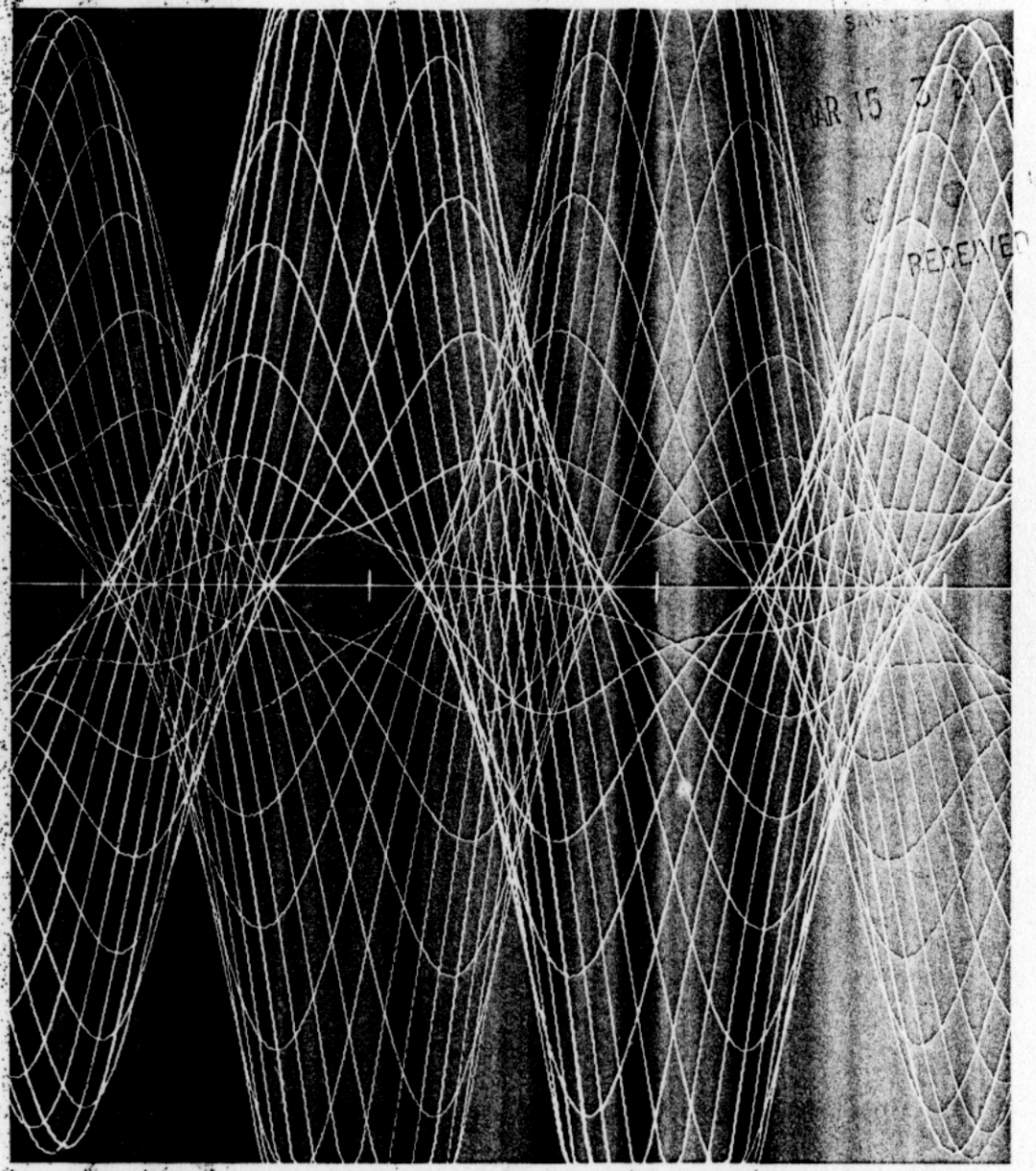

RJ 371

THEORY OF THE DETERMINATION OF THE OPTICAL CONSTANTS OF SEMICONDUCTOR THIN FILMS FROM PHOTOMETRIC MEASUREMENTS

Paul M. Grant

January 7, 1966

IBM RESEARCH

THEORY OF THE DETERMINATION OF THE OPTICAL CONSTANTS OF SEMICONDUCTOR THIN FILMS FROM PHOTOMETRIC MEASUREMENTS*

Paul M. Grant†

IBM San Jose Research Laboratory
San Jose, California

ABSTRACT: Theoretical studies have been carried out on the accuracy of derivation of the optical constants n and k of semiconductor thin films from photometric measurements in the critical point transition wavelength range 2000 - 6000Å. The two models explicitly considered were measurement of the normal incidence transmissivity and reflectivity of a single film and measurements of the transmissivity of two films of different thicknesses. Local inversion of the appropriate theoretical expressions was performed and the implicit derivatives $\partial n/\partial R$, $\partial n/\partial$. $\partial k/\partial R$, $\partial k/\partial T$ were calculated using germanium optical constants obtained by a Kramers-Kronig analysis of bulk reflectivity data. The film thicknesses considered were 50-500Å. The results indicate that in the wavelength regions where $n \approx k$, the error in the derived optical constants may become intolerably large for the usual experimental errors in the measured photometric intensities. It is concluded that such errors in n and k are inevitable for the class of valence semiconductors when measurements of normal incidence R and T are employed.

* Research supported by the Office of Naval Research.

† IBM Pre-doctoral Fellow. Division of Engineering and Applied Physics, Harvard University, Cambridge, Massachusetts.

Research Paper
RJ-371
January 7, 1966

I. INTRODUCTION

This paper deals with the theory of the deduction of the optical constants n and k from measurements of thin film photometric quantities such as reflectivity and transmissivity. High speed digital computers can be used to recover the optical constants from experimental values of R and T,[1-4] and results for epitaxial films of germanium on CaF_2 have been obtained.[5] It was found that there exists a region of high sensitivity to experimental error, especially when the optical constants are nearly equal and greater than unity. This sensitivity arises from the quadratic dependence of photometric intensities on the optical constants which creates at least one branch point upon attempting inversion. It is in the vicinity of these branch points that sensitivity to small changes in the intensities appear. We have made explicit calculations of this effect using optical constants of germanium determined from a dispersion analysis[6] of reflectivity data.[7] The results are given in Section III. Although we have used germanium as our calculational model, its optical constant structure is typical of a wide class of valence semiconductors[8] and deductions based on it will have wide qualitative application.[9]

II. THEORY

A modern discussion of the electromagnetic theory of light in a framework suitable for solids has been given by Stern.[10] We present here the results of applying this theory to the case of a thin absorbing film on a thick dielectric substrate. The reader interested in details should consult Refs. 1-4 and Refs. 9-10.

The film-substrate system considered is shown in Fig. 1. For plane waves impinging at normal incidence of the form:

$$\underset{\sim}{E} = \underset{\sim}{E}_o \, e^{i(\underset{\sim}{k}\cdot\underset{\sim}{r}-\omega t)} \tag{1a}$$

$$\underset{\sim}{H} = \underset{\sim}{H}_o \, e^{i(\underset{\sim}{k}\cdot\underset{\sim}{r}-\omega t)} \tag{1b}$$

where motion is in the direction of increasing $\underset{\sim}{r}$ and the wave vector $\underset{\sim}{k}$ in the film is defined by:

$$\underset{\sim}{k} \equiv (n + ik)(\omega/c)\underset{\sim}{1}_k \tag{2}$$

n and k being the real and imaginary parts of the complex index of refraction and $\underset{\sim}{1}_k$ the direction of propagation, the equations for the reflectivities and transmissivities given in Fig. 1 are as follows:

$$R_{FA} = R_{FA}^N\{[e^{\alpha a/2} - (R_{FS}^N/R_{FA}^N)^{1/2} e^{-\alpha a/2}]^2 + 4(R_{FS}^N/R_{FA}^N)^{1/2} \sin^2(\phi + [\psi_{FA}-\psi_{FS}]/2)\}/D \tag{3a}$$

$$R_{FS} = R_{FS}^N\{[e^{\alpha a/2} - (R_{FA}^N/R_{FS}^N)^{1/2} e^{-\alpha a/2}]^2 + 4(R_{FA}^N/R_{FS}^N)^{1/2} \sin^2(\phi + [\psi_{FA}-\psi_{FS}]/2)\}/D \tag{3b}$$

$$T_{FS} = 16n_s(n^2+k^2)/\{[(1+n)^2 + k^2][(n+n_s)^2 + k^2]D\} \tag{3c}$$

where:

$$D = [e^{\alpha a/2} - (R_{FA}^N R_{FS}^N)^{1/2} e^{-\alpha a/2}]^2 + 4(R_{FA}^N R_{FS}^N)^{1/2} \sin^2(\phi + [\psi_{FA}+\psi_{FS}]/2) \quad (3d)$$

$$R_{FA}^N = [(1-n)^2 + k^2]/[(1+n)^2 + k^2] \quad (3e)$$

$$R_{FS}^N = [(n_s-n)^2 + k^2]/[(n_s+n)^2 + k^2] \quad (3f)$$

$$\psi_{FA} = \arctan[2k/(n^2+k^2-1)] \quad (3g)$$

$$\psi_{FS} = \arctan[2n_s k/(n^2+k^2-n_s^2)] \quad (3h)$$

$$\alpha = 4\pi k/\lambda \quad (3i)$$

$$\phi = 2\pi na/\lambda \, . \quad (3j)$$

In Eqs. (3), n and k are the optical constants of the film, a its thickness, and n_s the index of refraction of the substrate. The index of refraction of air is taken as unity and λ is the wavelength referred to air. These equations apply only to films of isotropic, homogeneous, and non-magnetic materials. If the substrate were semi-infinite in extent, Eqs. (3) would be exact; however, we must in practice take account of the existence of a substrate-air interface. Harris, et al.,[2] have shown that this can be treated in a simple way by using intensity addition in the substrate. Assumptions necessary for the application of this technique imply an averaging process involving appropriate line-width and substrate thickness distribution functions such that phase interference is smoothed out. When these conditions hold, the following equations are obtained:

$$R = R_{FA} + T_{FS}^2 R_{AS}/(1 - R_{AS} R_{FS}) \quad (4)$$

$$T = T_{FS}(1 - R_{AS})/(1 - R_{AS} R_{FS}) \quad (5)$$

$$R' = R_{AS} + R_{FS}(1 - R_{AS})^2/(1 - R_{AS} R_{FS}) \quad (6)$$

where:

$$R_{AS} = (1 - n_s)^2/(1 + n_s)^2 \quad (7)$$

Here R is the total reflectivity for light incident from the left in Fig. 1, R' the total reflectivity for light incident from the right, and T is the total transmissivity for either direction. To find the effect of the finite substrate correction, we may take typically for germanium films in the visible $T_{FS} \approx 10^{-1}$, $R_{FS} \approx .50$, and $R_{AS} \approx .03$. This gives an additive factor 3×10^{-4} to R and a multiplicative factor .97 to T. Thus only the factor for T can be expected to amount to anything greater than experimental error for visible light. When the infrared transmission of a semiconductor film is used to determine its thickness, the factor .97 becomes important.

Figure 2 shows the optical constants of germanium derived by Philipp[6] from the reflectivity data of Donovan, et al.[7] for the wavelength range 2000-6000 Å. The result of substituting these constants into Eqs. (4) and (5) is given for T in Fig. 3 and for

R in Fig. 4. For CaF_2, n_s was taken from the supplier's manual.[11] The curves are calculated for films ranging in thickness from 50 Å to 500 Å in intervals of 50 Å. This covers the usable thickness range in which one can perform transmission experiments.

We now state two important approximations to Eqs. (4) and (5) to aid by qualitative discussion results to be derived numerically. The substrate backing will be neglected as it has no importance qualitatively. Thus (4) and (5) can be rewritten as:

$$R = R^N[(e^{\alpha a/2} - e^{-\alpha a/2})^2 + 4\sin^2\phi] / [(e^{\alpha a/2} - R^N e^{-\alpha a/2})^2 + 4R^N \sin^2(\phi + \psi)] \qquad (8)$$

$$T = 16(n^2+k^2)/[(1+n)^2 + k^2]^2 / [(e^{\alpha a/2} - R^N e^{-\alpha a/2})^2 + 4R^N \sin^2(\phi + \psi)] . \qquad (9)$$

One important approximation concerns the case where the absorption is strong enough to damp out interference effects. This occurs when $n \approx k$ and $e^{\alpha a} >> 4$, a good approximation in the wavelength region below 3500 Å for a 300 Å germanium film. Eqs. (8) and (9) then become:

$$R = R^N = [(1-n)^2 + k^2]/[(1+n)^2 + k^2] \qquad (10)$$

$$T = [(1-R)^2 + 4R \sin^2\psi]e^{-\alpha a} . \qquad (11)$$

If we further stipulate $k << n$ while keeping $e^{\alpha a} >> 4$, we obtain for (11):

$$T = (1-R)^2 e^{-\alpha a} . \qquad (12)$$

This form is particularly useful for the infrared spectroscopy of semiconductors and admits of an explicit solution for n and k:

$$k = \frac{\lambda}{4\pi a} \ln \frac{(1-R)^2}{T} \qquad (13)$$

$$n = \frac{1+R}{1-R} + \left\{ \frac{4R}{(1-R)^2} - \frac{\lambda^2}{16\pi^2 a^2} \left[\ln \frac{(1-R)^2}{T}\right]^2 \right\}^{1/2} . \qquad (14)$$

We stress, however, that some sort of numerical procedure is usually used and that (13) and (14) are very special cases. It is clear from (14) that a branch point exists in the solution for n, and that any pair of numbers R and T need not correspond to a real n. Thus errors in the experimental determination of R and T may lead to non-physical results. The criterion for real n can be written as an inequality between R and T:

$$T \geq (1-R)^2 \exp -\left[\frac{4\pi a}{\lambda} \frac{2\sqrt{R}}{1-R}\right] . \qquad (15)$$

If one plots (15) as an equality in a T vs. R representation, the T-R plane is essentially divided into two domains, one belonging to n real and the other n complex. Plotting the experimentally determined T and R for each wavelength on the same plane yields another curve. Whatever segment of this curve which crosses (15) into the complex n region determines the wavelength range for which no real n can be obtained from the experimental data using

Eqs. (10) and (12). Of course, if experimental conditions were such that the boundary conditions and assumptions leading to Eqs. (10) and (12) were obeyed exactly, and R and T measured perfectly, then such an intersection could never occur. Although in principle the inequality (15) cannot be violated, there is no reason why the discriminant of (14) cannot vanish if the optical constants permit. If this occurs, then there may exist a situation where small uncertainties in the experimental values of R and T will cause large uncertainties in n. Manipulation of Eqs. (10), (12), (13) and (14) yields:

$$n^2 = k^2 + 1 \tag{16}$$

as the condition for a vanishing discriminant. We observe that (16) violates one assumption, namely, $n \gg k$, necessary for the validity of Eq. (12). Nevertheless, we are encouraged to examine the consequences of Eq. (16) in more general circumstances when an explicit solution for n and k is not possible. If we examine the germanium optical constant curves of Fig. 2 we see that (16) is satisfied near $\lambda = 3000$ Å, and that the T vs. R plot of Fig. 5 for a 300 Å film indicates that near this wavelength small changes in the experimental values of R and T may determine whether or not n is real.

III. CALCULATIONS BASED ON THE GERMANIUM OPTICAL CONSTANTS

A. The Reflectivity-Transmissivity (RT) Method

The RT method for thin films obeying Eqs. (3), (4), and (5) will now be considered in detail. An explicit inversion as in (10) and (12) is not possible, and a numerical procedure must be invoked. However, regardless of the numerical operation used, it is important to know in principle how experimental errors in R and T affect the error in the derived optical constants. Therefore, consider the following first-order error differentials:

$$dn = \frac{\partial n}{\partial R}\,dR + \frac{\partial n}{\partial T}\,dT + \frac{\partial n}{\partial a}\,da \tag{17a}$$

$$dk = \frac{\partial k}{\partial R}\,dR + \frac{\partial k}{\partial T}\,dT + \frac{\partial k}{\partial a}\,da\ . \tag{17b}$$

It is to be remembered that in the mathematical context of the problem we treat R and T as the dependent variables, n and k as the independent variables, and a and λ as parameters. The partial derivatives of Eqs. (17) can only be calculated implicitly and to effect this, we use the following elementary operations of partial differential calculus:

$$\frac{\partial n}{\partial R} = \frac{\partial T}{\partial k}\Big/J \tag{18a}$$

$$\frac{\partial n}{\partial T} = -\frac{\partial R}{\partial k}\Big/J \tag{18b}$$

$$\frac{\partial k}{\partial R} = -\frac{\partial T}{\partial n}\Big/J \tag{18c}$$

$$\frac{\partial k}{\partial T} = \frac{\partial R}{\partial n}\Big/J \tag{18d}$$

$$\frac{\partial n}{\partial a} = (\frac{\partial R}{\partial k}\frac{\partial T}{\partial a} - \frac{\partial R}{\partial a}\frac{\partial T}{\partial k})/J \qquad (18e)$$

$$\frac{\partial k}{\partial a} = (\frac{\partial R}{\partial a}\frac{\partial T}{\partial n} - \frac{\partial R}{\partial n}\frac{\partial T}{\partial a})/J \qquad (18f)$$

where

$$J = \frac{\partial R}{\partial n}\frac{\partial T}{\partial k} - \frac{\partial R}{\partial k}\frac{\partial T}{\partial n} . \qquad (19)$$

The derivatives on the left-hand side of (18) will be called error derivatives, those on the right explicit derivatives. J is the Jacobian of the transformation. Since physical reasoning implies that R and T are rather smooth functions of n, k, and a, we may discount the explicit derivatives as contributing to singularities in the error derivatives, and conclude that such behavior will occur as $J \to 0$. It is instructive to examine briefly Eqs. (18) and (19) applied to the approximate Eqs. (10) and (12). The explicit derivatives are:

$$\frac{\partial R}{\partial n} = 4(n^2 - k^2 - 1)/[(1+n)^2 + k^2]^2 \qquad (20a)$$

$$\frac{\partial R}{\partial k} = 8nk/[(1+n)^2 + k^2]^2 \qquad (20b)$$

$$\frac{\partial T}{\partial n} = -32e^{-\alpha a}\, n^2(n^2 - k^2 - 1)/[(1+n)^2 + k^2]^3 \qquad (20c)$$

$$\frac{\partial T}{\partial k} = -64e^{-\alpha a}\, n^2\left[k + \frac{\pi a}{\lambda}[(1+n)^2 + k^2]\right] /[(1+n)^2 + k^2]^3 \qquad (20d)$$

$$\frac{\partial R}{\partial a} = 0 \qquad (20e)$$

$$\frac{\partial T}{\partial a} = -\frac{64\pi n^2 k}{\lambda} e^{-\alpha a}/[(1+n)^2 + k^2]^2 \qquad (20f)$$

$$J = -\frac{256\pi a}{\lambda} e^{-\alpha a}\, n^2(n^2 - k^2 - 1)/[(1+n)^2 + k^2]^4 . \qquad (20g)$$

The corresponding error derivatives are:

$$\frac{\partial n}{\partial R} = \left\{\frac{\lambda k}{\pi a} + [(1+n)^2 + k^2]\right\}[(1+n)^2 + k^2]/4(n^2 - k^2 - 1) \qquad (21a)$$

$$\frac{\partial n}{\partial T} = \frac{\lambda k}{\pi a}[(1+n)^2 + k^2]^2\, e^{\alpha a}/32n(n^2 - k^2 - 1) \qquad (21b)$$

$$\frac{\partial k}{\partial R} = -\frac{\lambda}{8\pi n a}[(1+n)^2 + k^2] = -\frac{\lambda}{2\pi a(1-R)} \qquad (21c)$$

$$\frac{\partial k}{\partial T} = -\frac{\lambda}{64\pi n^2 a}[(1+n)^2 + k^2]^2\, e^{\alpha a} = -\frac{\lambda}{4\pi a T} \qquad (21d)$$

$$\frac{\partial n}{\partial a} = 2nk^2/a(n^2 - k^2 - 1) \qquad (21e)$$

$$\frac{\partial k}{\partial a} = -k/a . \qquad (21f)$$

We see that (20g) vanishes for $n^2 = k^2 + 1$ and causes singularities in the error derivatives $\partial n/\partial R$, $\partial n/\partial T$, and $\partial n/\partial a$. The quantities $\partial k/\partial R$, $\partial k/\partial T$, and $\partial k/\partial a$ remain unaffected. These results are directly related to the fact that, according to Eqs. (13) and (14), a branch point exists only in n and not k when $n_1^2 = k^2 + 1$.

Before proceeding further, we make some general comments concerning the geometrical interpretation of J. Consider Eqs. (4) and (5) in the form:

$$R(n,k) - R = 0 \qquad (22)$$

$$T(n,k) - T = 0 \tag{23}$$

where R and T are the experimentally determined quantities. It is apparent that each equation determines a separate functional dependence of the optical constants on one another. That is, for (22) we can write:

$$n = n_R(k) \tag{24}$$

and for (23):

$$n = n_T(k) . \tag{25}$$

Equations (24) and (25) will be called root-locus equations and their points of intersection in the n-k plane determine the simultaneous solutions of Eqs. (22) and (23). For example, the root-locus of (10) is a circle of radius $2\sqrt{R}/(1-R)$ and center at $n = (1+R)/(1-R)$, $k = 0$. On the other hand, the root-locus of (11) or (12) has no simple form. However, if the absorption is high enough, n has roughly a decaying exponential dependence on k. By using the definition of the vector product, we can form:

$$\sin\theta_{RT} = \left|\frac{\nabla R \times \nabla T}{|\nabla R||\nabla T|}\right| = \frac{J}{\left\{\left[\left(\frac{\partial R}{\partial n}\right)^2 + \left(\frac{\partial R}{\partial k}\right)^2\right]\left[\left(\frac{\partial T}{\partial n}\right)^2 + \left(\frac{\partial T}{\partial k}\right)^2\right]\right\}^{1/2}} . \tag{26}$$

Hence when $J=0$, $\theta_{RT} = 0$, or (24) becomes tangent to (25) thus leading to a highly unstable condition with regard to experimental errors in R and T. If the errors are such as to prevent any intersection or tangency at all, then we obtain no real roots. This is the analogy for the general case to the special case of Eqs. (10) and (12) when the discriminant of (14) goes negative.

Figures 6, 7, 8, and 9 depict the root-locus diagrams for germanium films on CaF_2 substrates for thicknesses of 50 Å, 150 Å, 300 Å, and 500 Å, respectively. Three representative wavelengths, namely, 2500 Å, 3000 Å, and 5500 Å, are plotted for each thickness with the exception of the 300 Å case where 3900 Å is given also. These curves were calculated by using data from Refs. 6 and 11 in conjunction with Eqs. (3), (4), and (5). We note that there is usually more than two simultaneous solutions to Eqs. (24) and (25); in fact, because of interference effects the actual number is indeterminate. However, we observe that all but one solution changes with thickness at a given wavelength. This solution is obviously the physical one and the one given by the dispersion relations also. For the most part, the root-locus curves of Figs. 6-9 have the qualitative behavior suggested by the root-loci of (10) and (12) except that $n_R(k)$ has multiple "loops" because of phase interference. Note that near $\lambda = 3000$ Å for all thicknesses one finds $n_R(k)$ almost tangent to $n_T(k)$. It is easy to see that small variations in the experimental R and T can cause large variations in the deduced n and k, especially n. The value $\lambda = 3000$ Å was also obtained from the simple model of Eqs. (10) and (12), even though $n^2 = k^2+1$ violates one of the assumptions of its derivation. That interference and absorption

are not entirely without their effects is demonstrated by the 300 Å film for λ = 3900 Å, where a condition of near tangency exists for $n^2 \neq k^2+1$ (see Fig. 8d).

Figures 10, 11, and 12 present θ_{RT} and the magnitude of the error derivatives as functions of wavelength for the four thicknesses mentioned above. They confirm in detail previous discussion of the root-locus diagrams. It is seen that for short wavelengths the behavior is fairly independent of thickness, except for 300 Å where the singularity is shifted to longer wavelengths, probably because of an interference effect. Note that the model of Eqs. (3), (4), and (5) leads to singularities in all error derivatives.

In order to gain some feeling for the wavelength ranges over which reasonable experimental errors in R, T, and a would lead to unreasonable errors in n and k, the bar diagrams Figs. 13, 14, and 15 were constructed. The choice of a reasonable experimental error is somewhat arbitrary; however, one can generally conclude that an absolute error in n and k of no greater than 0.5 is necessary if one is to approach the accuracy of the dispersion analyses. Experience suggests we assign an absolute error of ±2.5% to R, a relative error of ±10% to T, and an absolute error of ±10 Å to a. The last figure is probably optimistic. These criteria result in the minimal values of the error derivatives indicated on the bar diagrams. There are two important conclusions to be drawn from Figs. 13-15. The first is that an optimum thickness range exists in which to choose films for the determination of optical constants, and the second is that there is no way in which one may choose two films of different thicknesses in an attempt to circumvent the troublesome wavelength range.

B. The Two Thickness, Two Transmission Method

There are photometric techniques other than the RT method by which the deduction of the optical constants can be effected. Any method which involves measurement of two independent intensities can be considered; for example:

(a) measurement of R (Eq. (4)) and R' (Eq. (6)),

(b) measurement of R, T, R' to obtain n, k, and a,

(c) measurement of the reflectivity at two angles of incidence, and

(d) measurement of the transmissivity of two films of different thicknesses.

These and others are discussed by Heavens.[12] Because it turns out that transmissivity measurements are usually easier to make, we will consider method (d) as an alternative to the RT method. Method (d) assumes that n and k are independent of a, an assumption that should be justified for epitaxial films of thickness greater than about 25 interatomic distances, but may not hold for films of unknown crystalline perfection.

The two thickness, two transmission method was the approach used by Brattain and Briggs[13] and Gebbie[14] to obtain the optical constants of germanium films. The appropriate equations are:

$$T = T(n,k;\lambda;a) \tag{27}$$

$$T' = T(n,k;\lambda;a') \tag{28}$$

where the functional dependence of the right hand side is given by Eqs. (3) and (5). The appropriate error differentials are:

$$dn = \frac{\partial n}{\partial T}\,dT + \frac{\partial n}{\partial T'}\,dT' + \frac{\partial n}{\partial a}\,da + \frac{\partial n}{\partial a'}\,da' \tag{29}$$

$$dk = \frac{\partial k}{\partial T}\,dT + \frac{\partial k}{\partial T'}\,dT' + \frac{\partial k}{\partial a}\,da + \frac{\partial k}{\partial a'}\,da' \ . \tag{30}$$

Calculations with the germanium data show that the extinction coefficient error derivatives have no singularities and are too small to cause an error of ±0.5 in the optical constants at any wavelength. We thus consider only the index of refraction errors. It is likely that any relative errors in the measurement of the two transmissivities will be systematic. That is, it is found experimentally that most errors in measuring transmission are due to misalignment and substrate refraction which will be common to all samples. Therefore, for the purpose of condensing the results, we posit $dT/T \approx dT'/T'$ which permits us to consider the single quality $|T(\partial n/\partial T) + T'(\partial n/\partial T')|$. However, it usually turns out that $T(\partial n/\partial T)$ and $T'(\partial n/\partial T')$ are nearly equal in magnitude but opposite in sign; therefore, the results presented here may unrealistically favor the two thickness, two transmission method. It often happens that $T(\partial n/\partial T)$ and $T'(\partial n/\partial T')$ are by themselves more than large enough to cause errors >0.5 in n but their sum causes almost complete cancellation. It is also assumed that we can combine the thickness induced errors into a single quantity $|(\partial n/\partial a) + (\partial n/\partial a')|$ by considering $da \approx da'$. The experimental motivation in this case, however, is less clear than in the former, although if the thickness is measured by infrared transmission, the justification becomes the same as above. Again the two thickness, two transmission method may seem unduly favored because $|\partial n/\partial a| \approx |\partial n/\partial a'|$ with their signs opposing. Figures 16 and 17 show the behavior of the combined error derivatives with wavelength. They are plotted as a family of curves for representative thickness pairs. Note that, although there are no singularities in the region near $n^2 = k^2+1$, almost every curve has a relative maximum in this area.

We see from Figs. 16 and 17 that it is possible to choose an optimum thickness pair for which the effect of experimental errors will be minimized. In fact, for a = 100 Å, a' = 300 Å or 400 Å, the combined error derivatives have values below the limits imposed by discussions above. Therefore, it appears that a judicious choice of film pairs could yield reasonably accurate values of the optical constants.

IV. CONCLUSIONS

Historically optical constants obtained from thin film measurements have been held to represent only the optical properties of a particular film formed under certain conditions and

not necessarily correlated with bulk properties. The availability of epitaxial films makes it more likely that the deduced optical constants are also those of bulk material. A firm knowledge of the constants obtained from bulk reflectivity measurements now enables us to test for film conditions that minimize experimental and interpretive errors.

For the RT method, it has been shown that there exists a range of thicknesses for which intolerable sizes of the error derivatives are limited to a minimum wavelength range. However, for the thicknesses under consideration here there will always be some wavelength range in which the error derivatives are very large. Such will very likely be the case for most semiconductor materials. Table I gives the energy and wavelength at which $n^2 = k^2+1$ for several well-known semiconductors. Although this table is incomplete, similarities in band structure lead one to conclude $n^2 = k^2+1$ at some wavelength for all the usual valence semiconductors. The condition $n^2 = k^2+1$ can be written as $\varepsilon_1 = 1$ or $\chi_1 = 0$ in terms of the dielectric constant or susceptibility, respectively. If we assume that all critical point transitions between the valence bands and excited states (conduction bands) can be expressed in terms of a single frequency ω_0 suitably broadened by an appropriate lifetime-like parameter τ, then χ_1 takes the form:

$$\chi_1 = A \frac{\omega_0^2-\omega^2}{(\omega_0^2-\omega^2)^2 + \omega^2/\tau^2} + \chi_d(\omega) + \chi_c(\omega) \qquad (31)$$

where ω is the frequency of the incident photons. The susceptibilities $\chi_d(\omega)$ and $\chi_c(\omega)$ express the dependence on d-band and core state transitions respectively. For ω in the critical point transition range, $\chi_d(\omega)$ and $\chi_c(\omega)$ are small compared to the first term in (31) everywhere except for ω near ω_0. These terms have the effect of shifting the zero crossing of χ_1 to a value of $\omega > \omega_0$. However, because of the large energy difference between the critical point transitions on the one hand and the d-band and core state transitions on the other, this shift should only be a small amount. Therefore, it appears there will invariably be a branch point in the RT method occurring somewhere in the vicinity of the critical point transitions.

However, it seems possible with the two transmission, two thickness method to circumvent this difficulty. On the other hand, it was pointed out that our method of presentation would probably favor this technique. Similar analyses should be undertaken for other photometric methods to judge the efficacy of each for calculating optical constants from film data. The results for the RT method and the two thickness, two transmission method argue eloquently for the necessity of investigating in detail whatever other methods may be chosen in order that experimental conditions may be arranged for optimum results.

ACKNOWLEDGEMENTS

The author would like to express his gratitude to Professor William Paul for guidance and criticism throughout the course of this work. He also wishes to extend his thanks to C. E. Rossi and B. B. Kosicki for valuable discussions on the content of this paper and acknowledge several useful conservations with J. R. Dixon and R. B. Schoolar on lead salt film optical constant work being done at the U.S. Naval Ordnance Laboratory.

Several weeks after delivering a talk on the subject matter of this paper,[9] the author received a letter from Professor F. Abelès informing him of some theoretical work done by one of his students on this problem.[16] The author wishes to acknowledge this and thank Professor Abelès for bringing this work to his attention.

Some of the calculations in this paper were performed under a grant from the MIT Computation Center.

REFERENCES

1. L. Harris and A. L. Loeb, J. Opt. Soc. Am. 45, 179 (1955).
2. L. Harris, J. K. Beasley, and A. L. Loeb, J. Opt. Soc. Am. 41, 604 (1951).
3. A. L. Loeb and H. H. Denman, J. Soc. Indust. Appl. Math. 3, 1 (1955).
4. J. F. Hall and W. F. C. Ferguson, J. Opt. Soc. Am. 45, 714 (1955).
5. P. M. Grant, to be published in J. Appl. Phys.; P. M. Grant, Bull. Am. Phys. Soc. 10, Series II, 1185 (1965).
6. H. R. Philipp, private communication.
7. T. M. Donovan, E. J. Ashley, and H. E. Bennett, J. Opt. Soc. Am. 53, 1403 (1963).
8. H. R. Philipp and H. Ehrenreich, Phys. Rev. 129, 1550 (1963).
9. P. M. Grant, Bull. Am. Phys. Soc. 10, Series II, 546 (1965); P. M. Grant, Gordon McKay Laboratory of Applied Science, Harvard University, Technical Report HP-14, 1965 (unpublished), CFSTI #AD-619071.
10. F. Stern, Elementary Theory of the Optical Properties of Solids, Solid State Physics, Vol. 15, ed. by F. Seitz and D. Turnbull (Academic Press, New York, 1963).
11. Optovac Optical Crystals Bulletin No. 50, Optovac, Inc., North Brookfield, Mass.
12. O. S. Heavens, Optical Properties of Thin Solid Films (Butterworths Scientific Publications, London, 1953); O. S.

Heavens, Measurement of Optical Constants of Thin Films, Physics of Thin Films, Vol. 2, ed. by G. Hass and R. E. Thun (Academic Press, New York, 1964).

13. W. H. Brattain and H. B. Briggs, Phys. Rev. 75, 1705 (1949).

14. H. A. Gebbie, Ph.D. Thesis (unpublished), Reading, 1952; according to Ref. 12, Optical Properties of Thin Solid Films, p. 137.

15. M. Cardona and D. L. Greenaway, Phys. Rev. 133, A1685 (1964).

16. C. Bazin, C. R. Acad. Sc. Paris 260, 83 (1965).

Table I. Wavelength and energy at which $n^2 = k^2+1$ or $\epsilon_1 = 1$ for several common semiconductor materials.

Material	Energy (eV)	Wavelength (Å)
Ge	4.13	3000
Si[a]	4.0	3100
InSb[a]	3.8	3250
InAs[a]	4.5	2750
GaAs[a]	4.7	2650
GaP[a]	5.1	2450
PbS[b]	3.1	4000
PbTe[b]	1.8	6900
PbSe[b]	2.2	5650

a. See Ref. 8.

b. See Ref. 15.

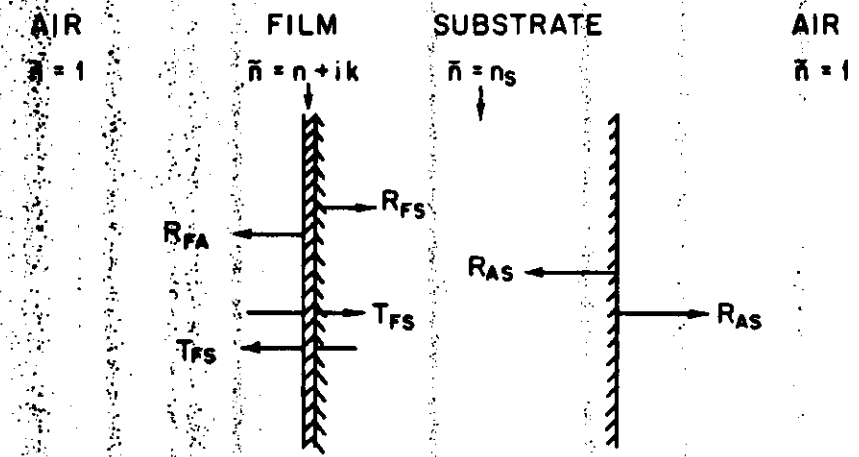

Figure 1 Intensity addition model for a thin absorbing film on a thick non-absorbing substrate.

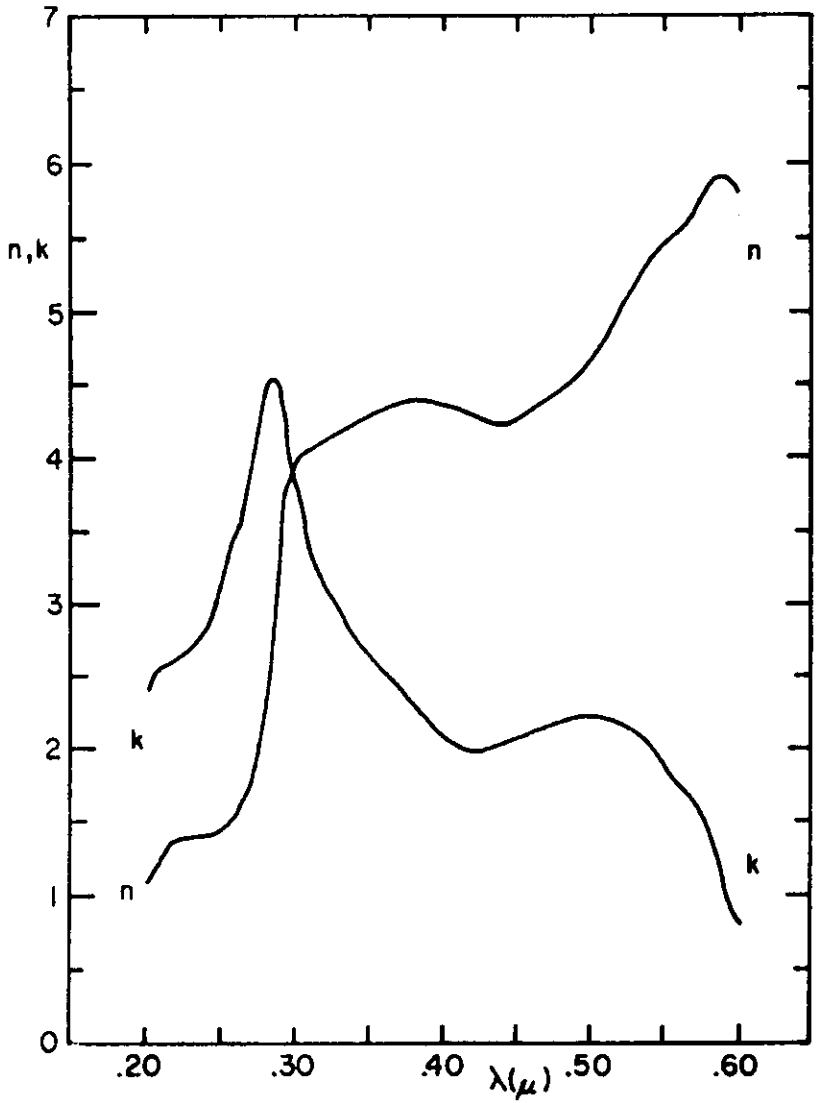

Figure 2 Optical constants of germanium calculated by a Kramers-Kronig analysis of bulk single crystal reflectivity data. See Refs. 6 and 7.

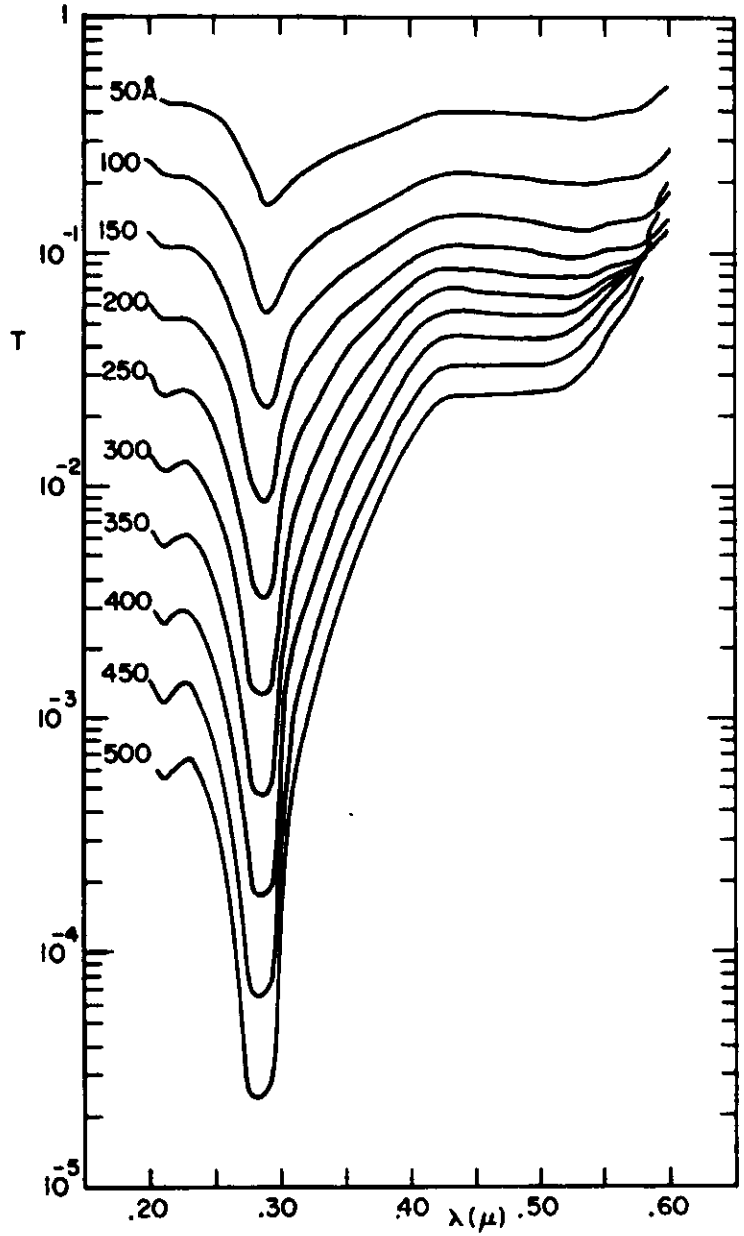

Figure 3 Transmission of germanium thin films on CaF_2 calculated from the data of Figure 2. Film thickness is indicated on each curve.

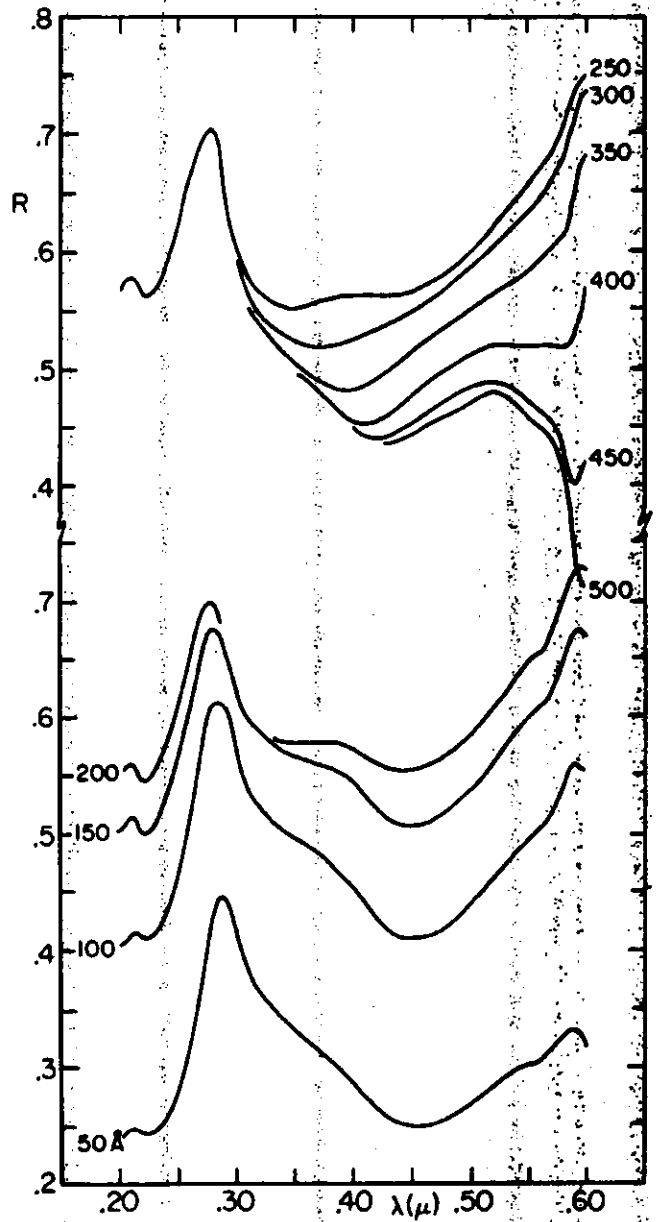

Figure 4 Reflectivity of germanium thin films on CaF_2 calculated from the data of Figure 2. Film thickness is indicated on each curve.

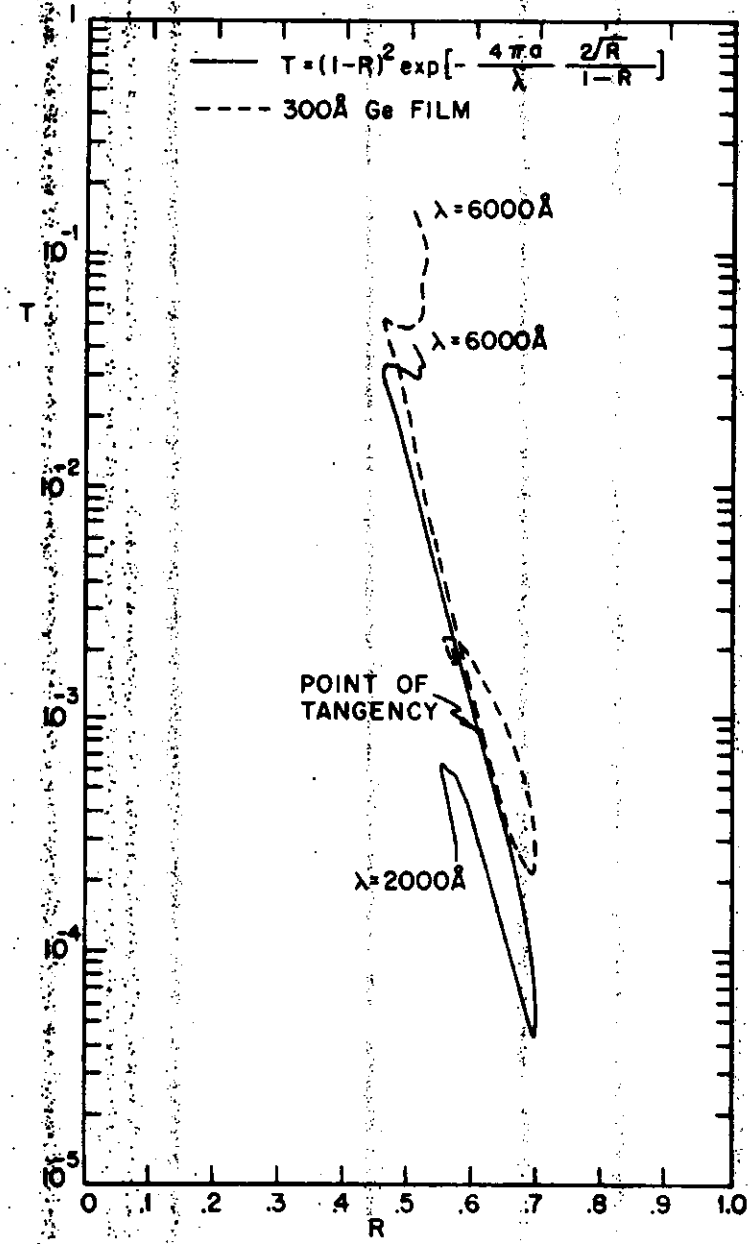

Figure 5. A T vs. R representation using Eq. (15) and R and T for a 300Å Ge film calculated from Eqs. (10) and (12).

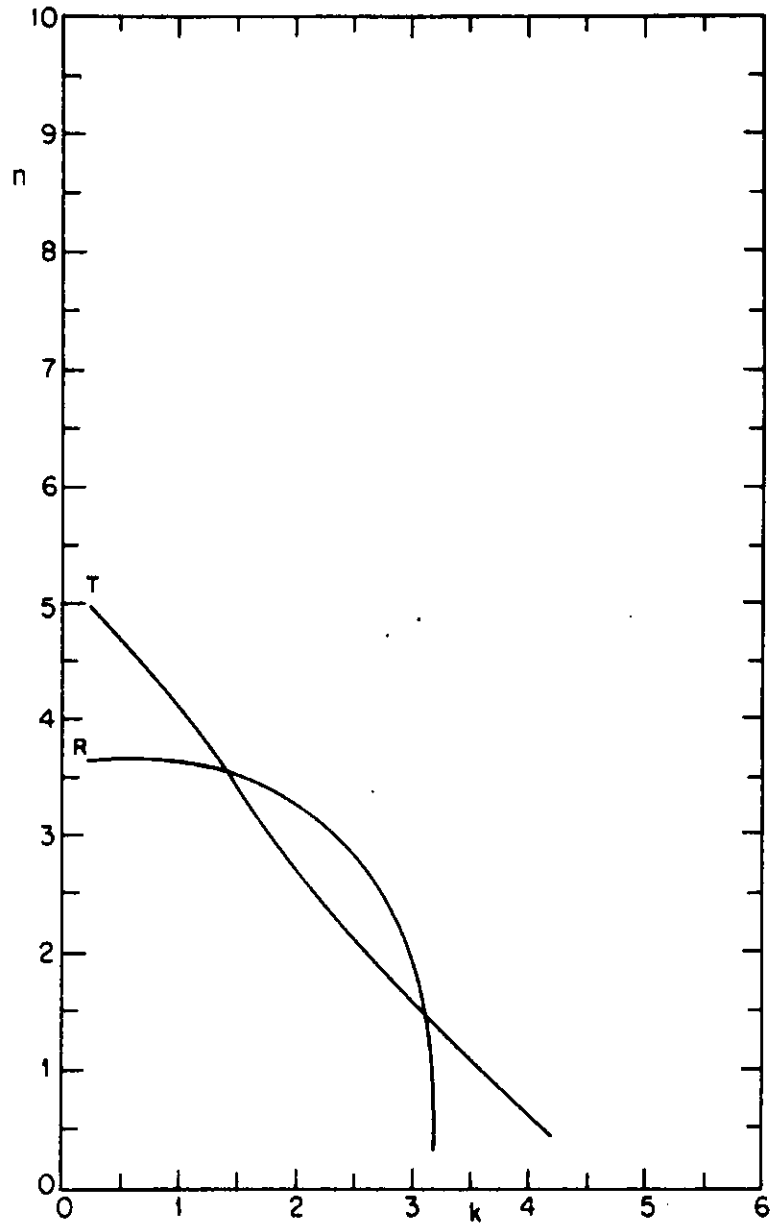

Figure 6a Root-locus diagram of a 50Å Ge film on a CaF_2 substrate. $\lambda = 2500Å$.

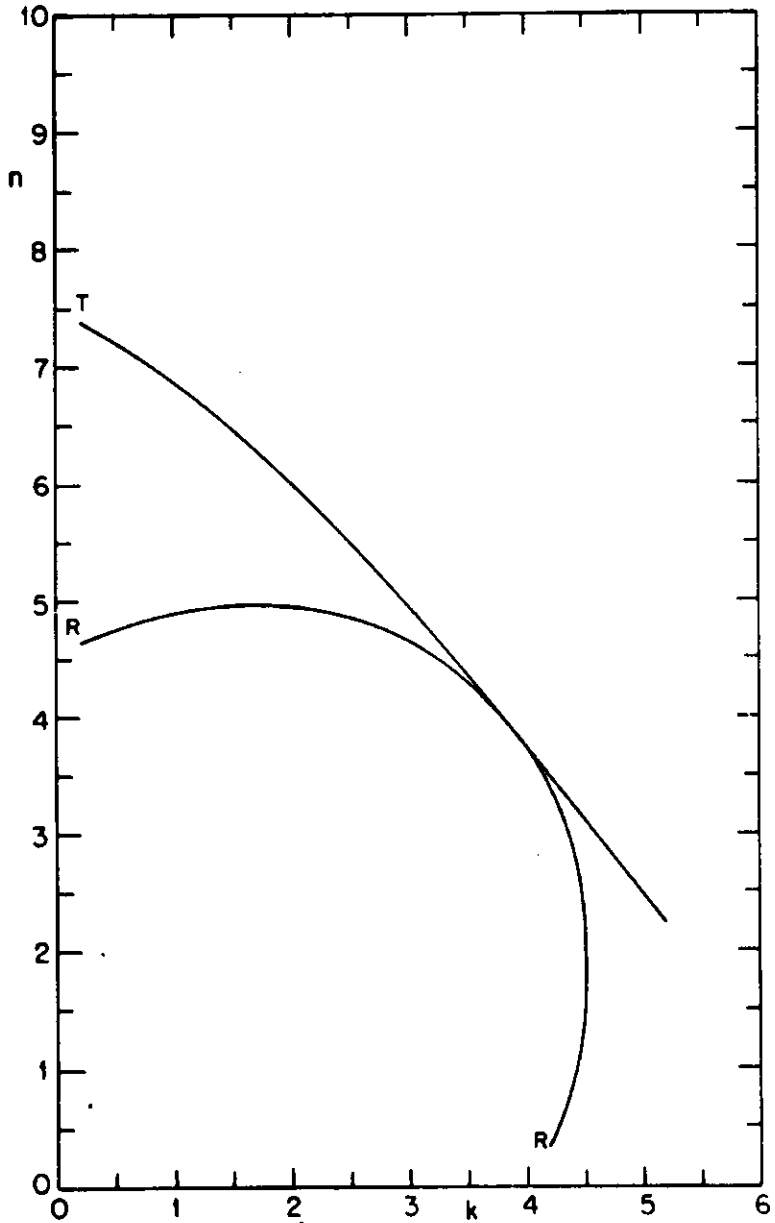

Figure 6b $\lambda = 3000\text{Å}$, $a = 50\text{Å}$.

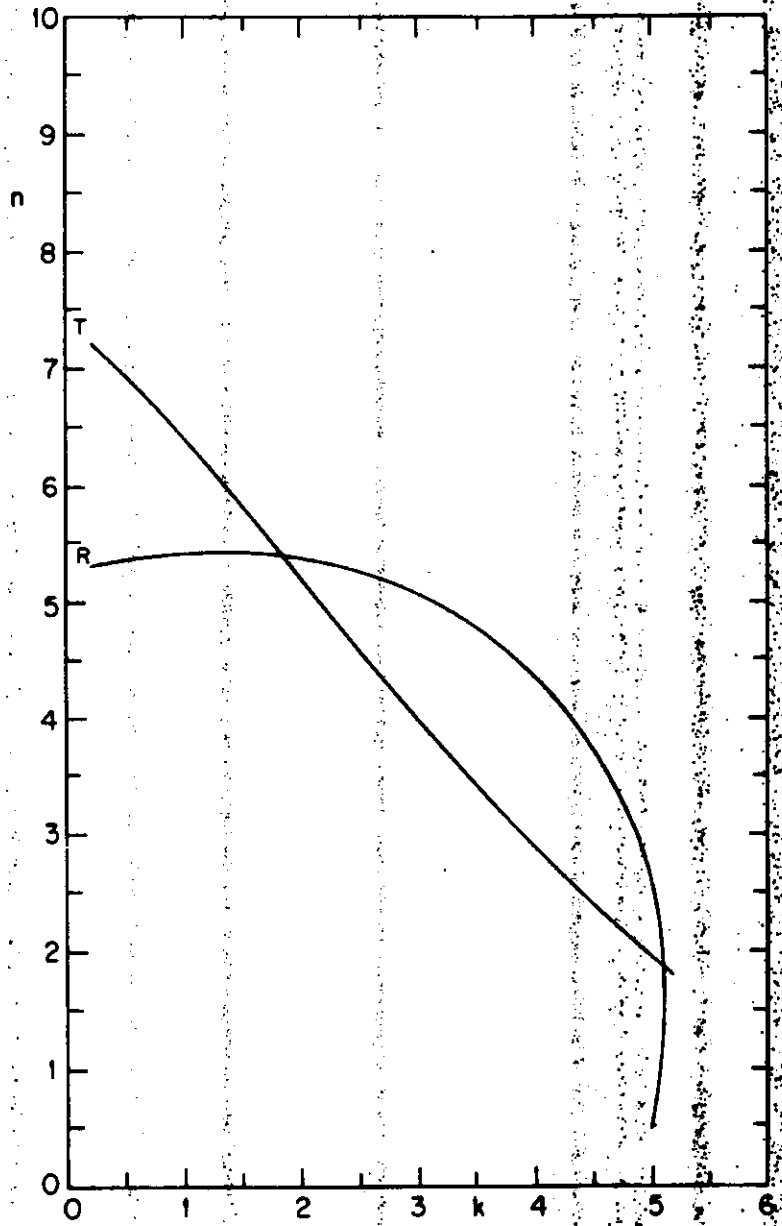

Figure 6c $\lambda = 5500\text{Å}$, $a = 50\text{Å}$.

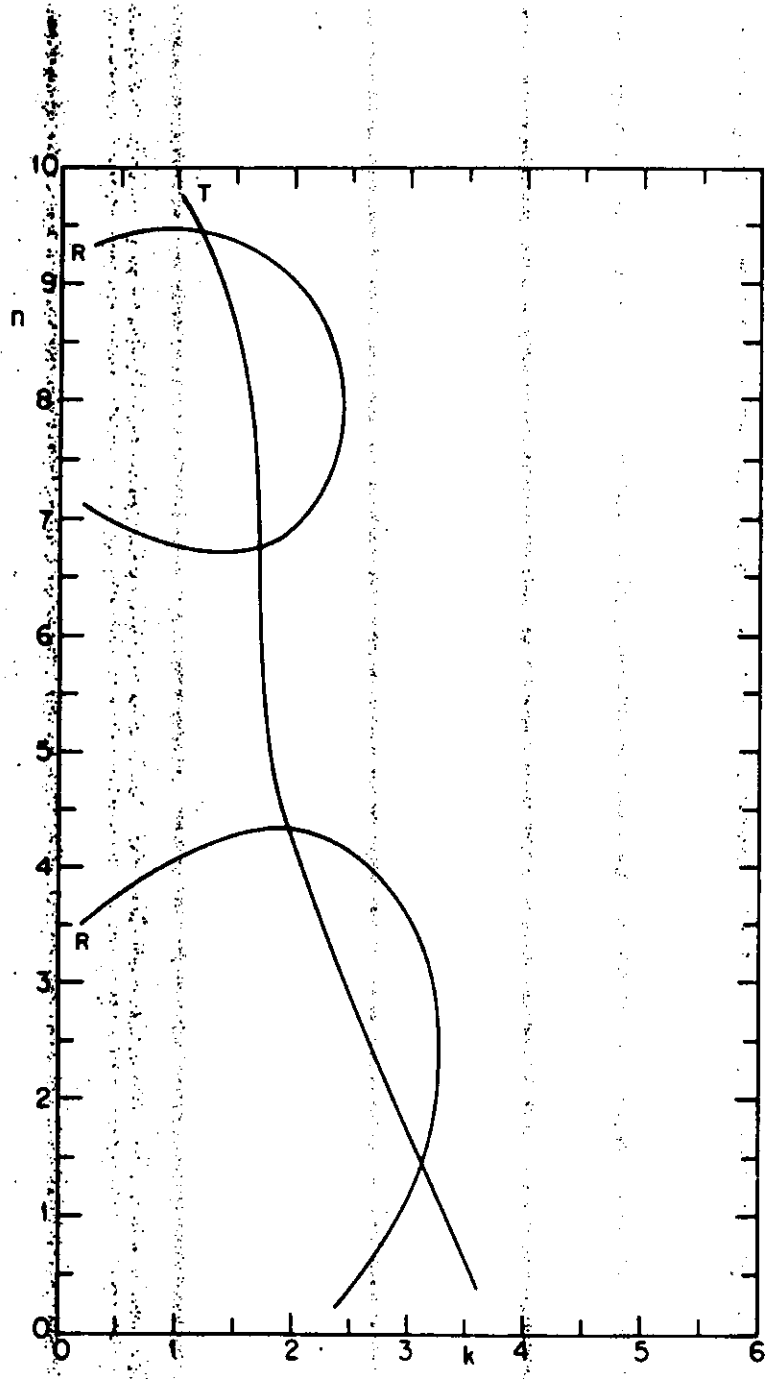

Figure 7a Root-locus diagram of a 150Å Ge film on a CaF_2 substrate. $\lambda = 2500$Å.

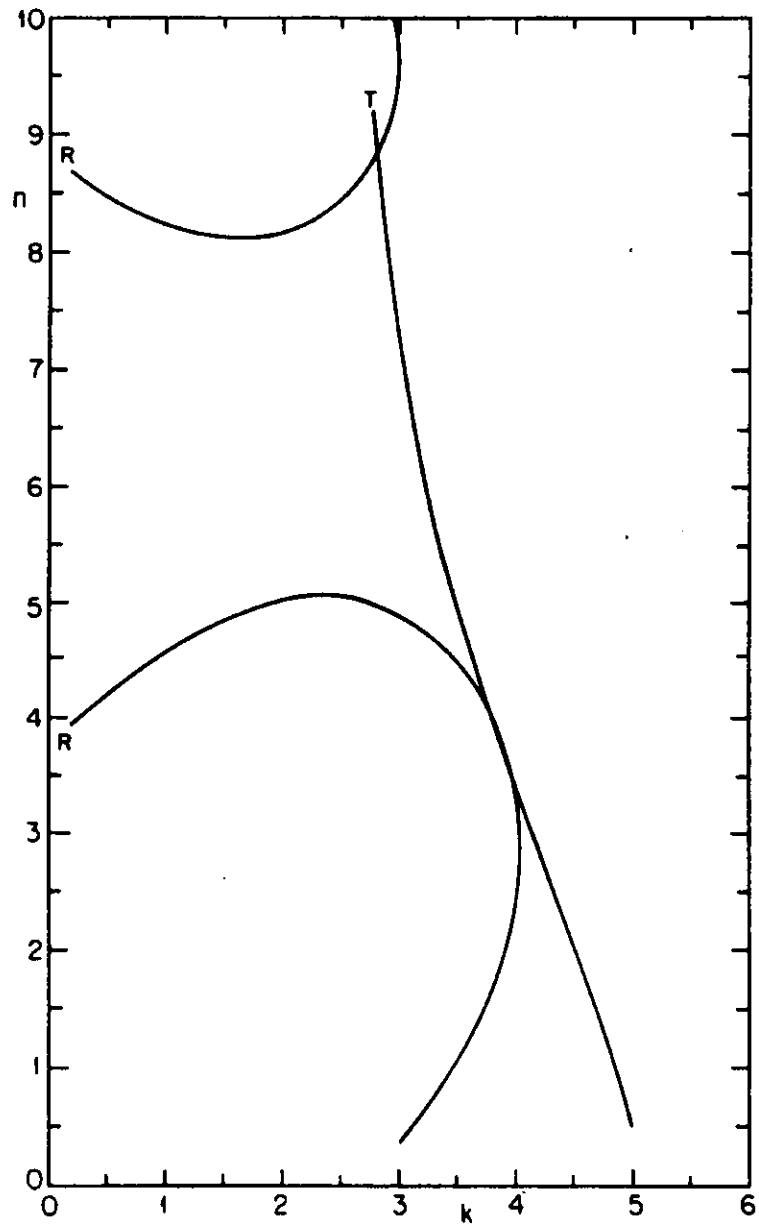

Figure 7b $\lambda = 3000$Å, $a = 150$Å.

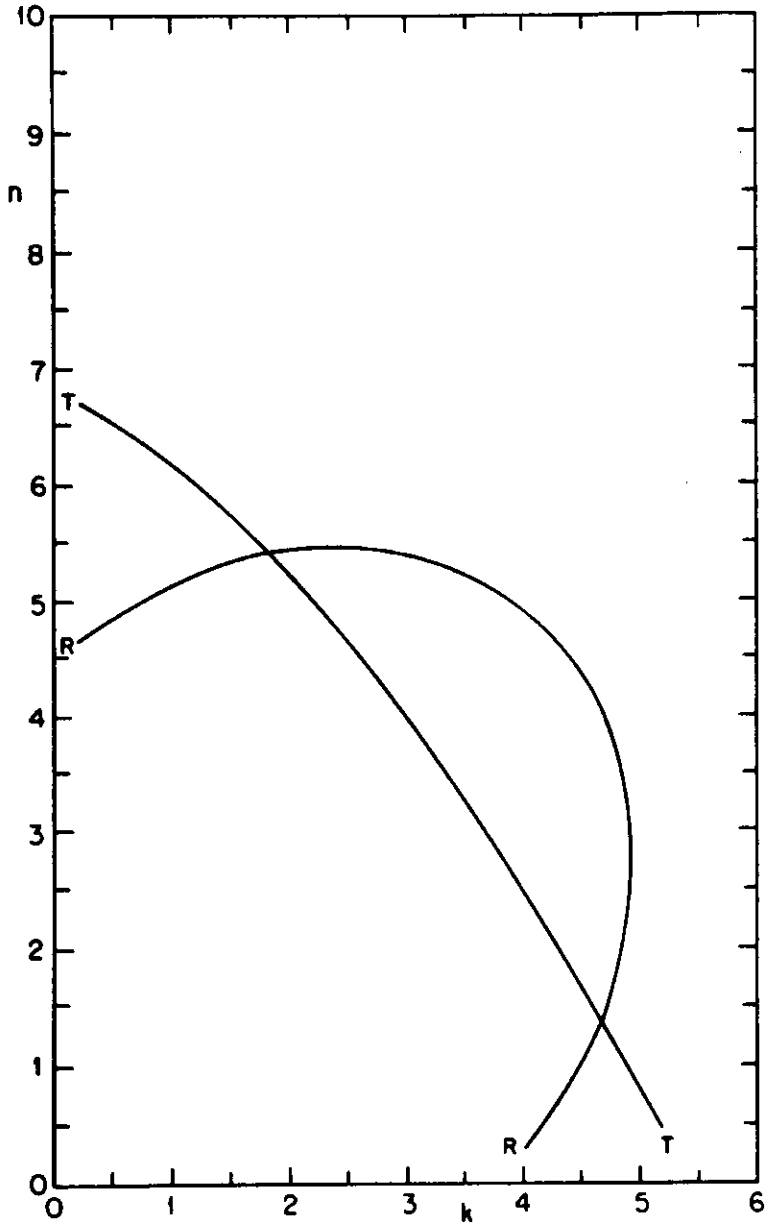

Figure 7c $\lambda = 5500$Å, $a = 150$Å.

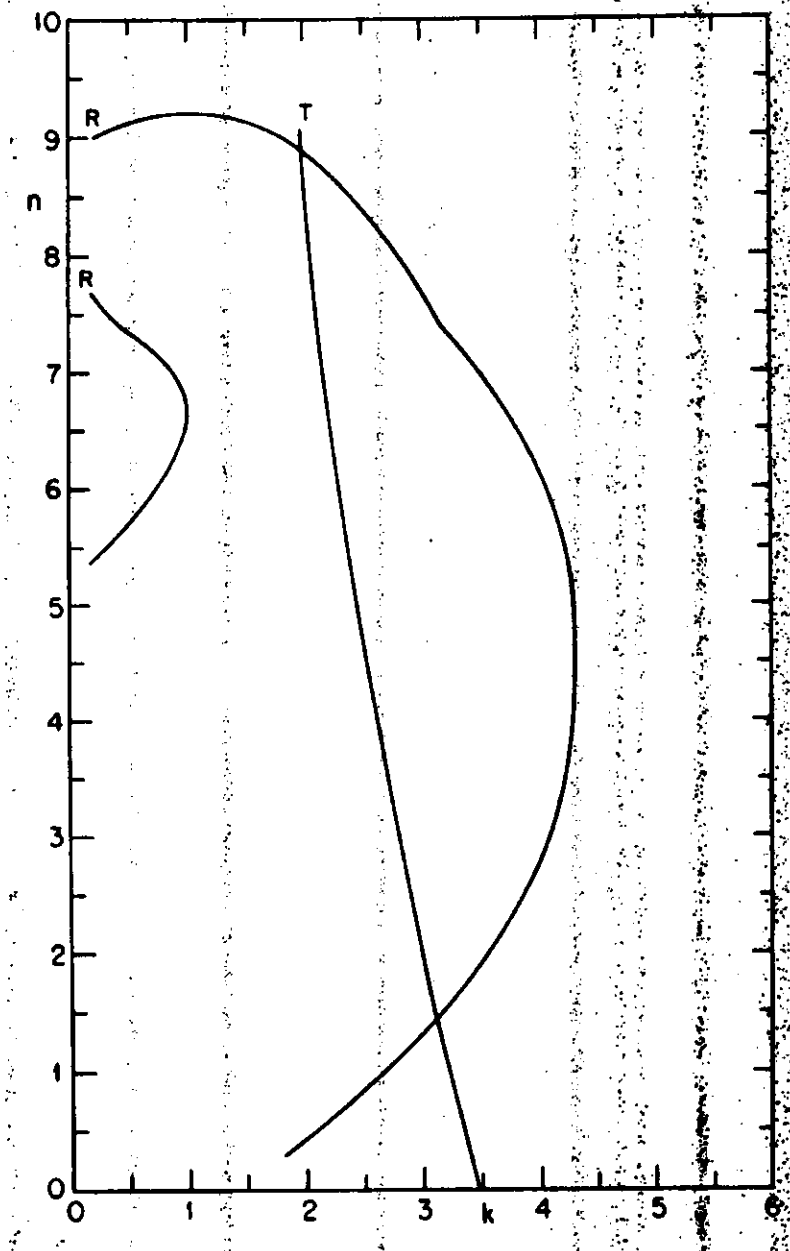

Figure 8a Root-locus diagram of a 300Å Ge film on a CaF_2 substrate. $\lambda = 2500$Å.

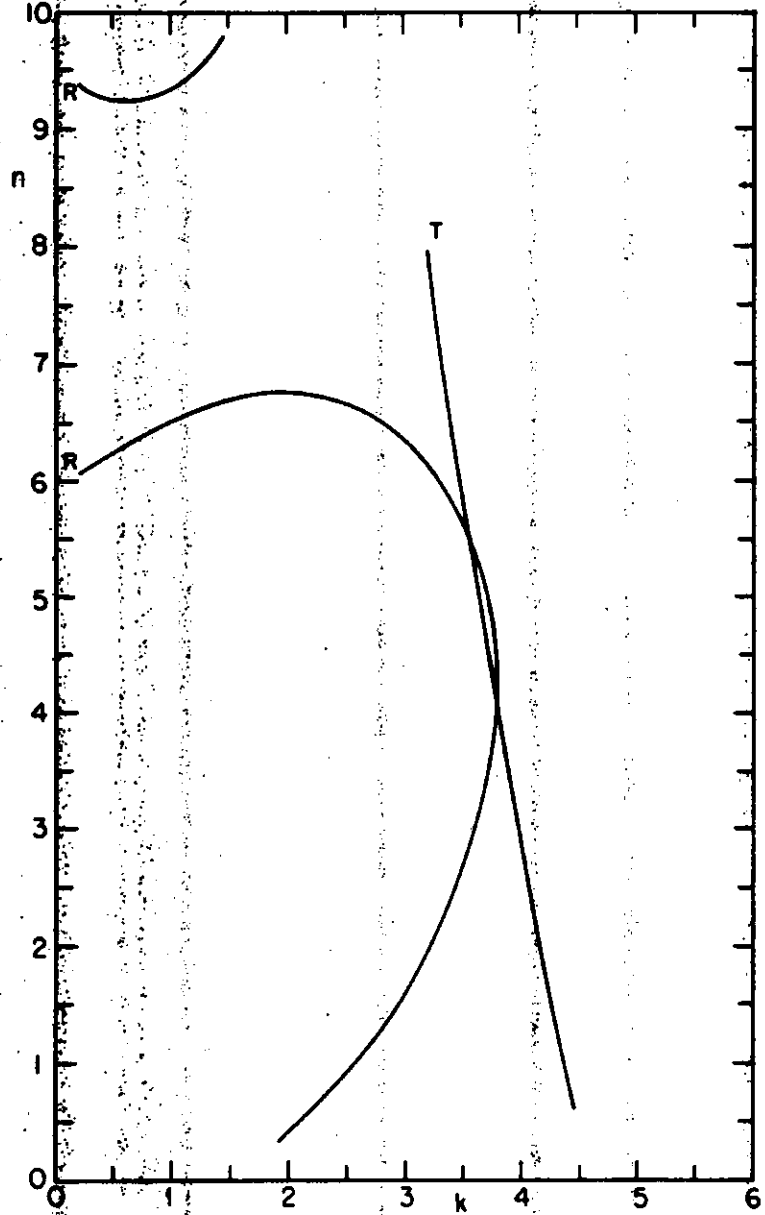

Figure 8b $\lambda = 3000\text{Å}$, $a = 300\text{Å}$.

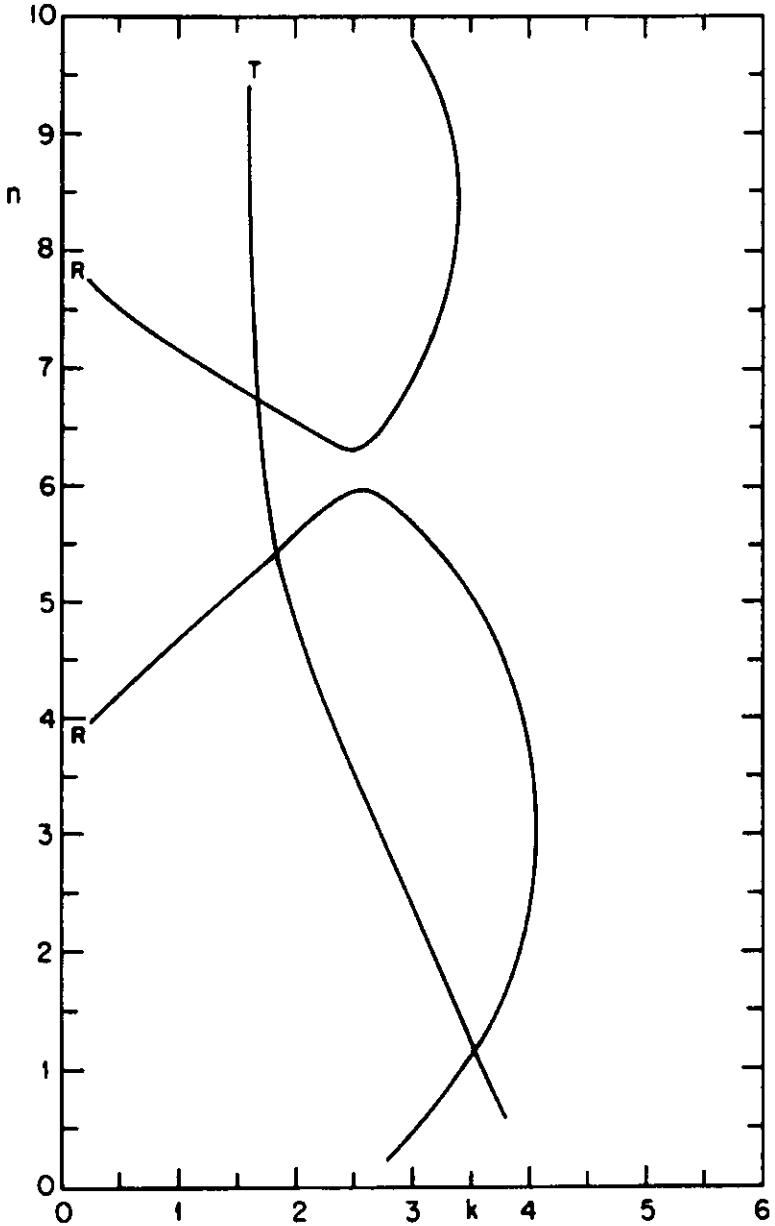

Figure 8c $\lambda = 5500\text{Å}$, $a = 300\text{Å}$.

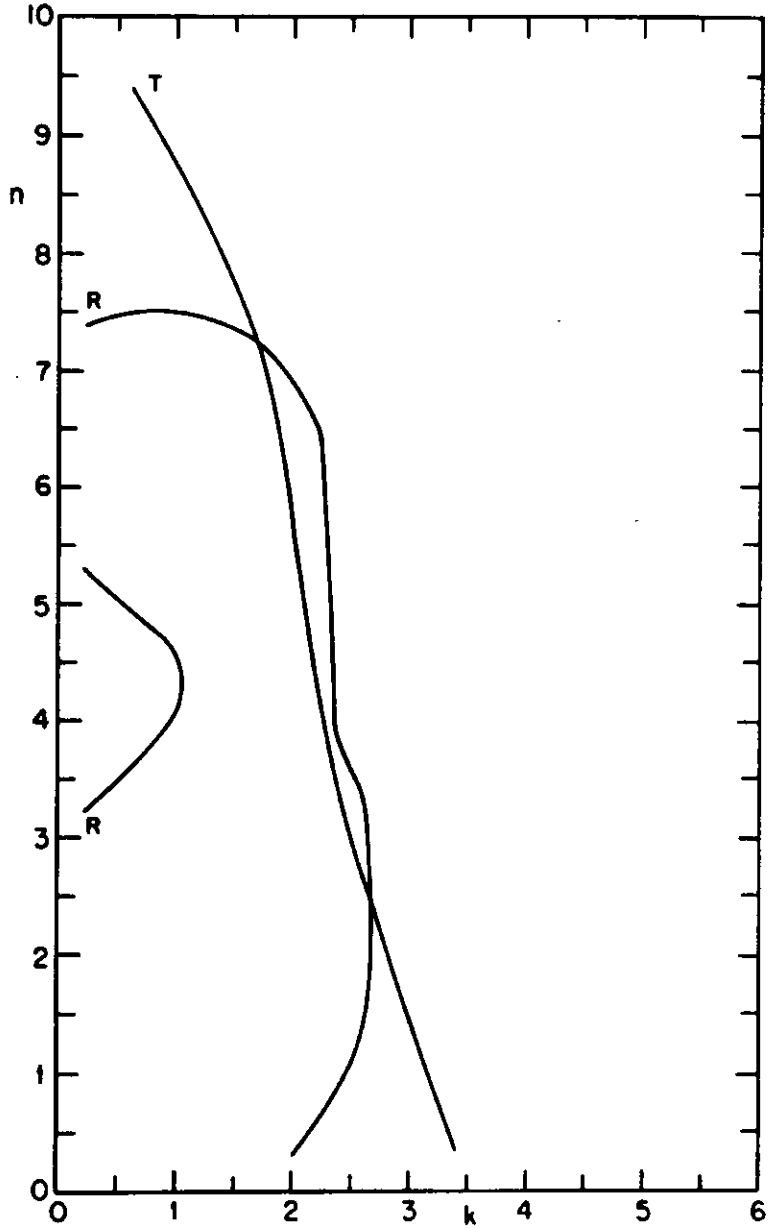

Figure 8d $\lambda = 3900$Å, $a = 300$Å.

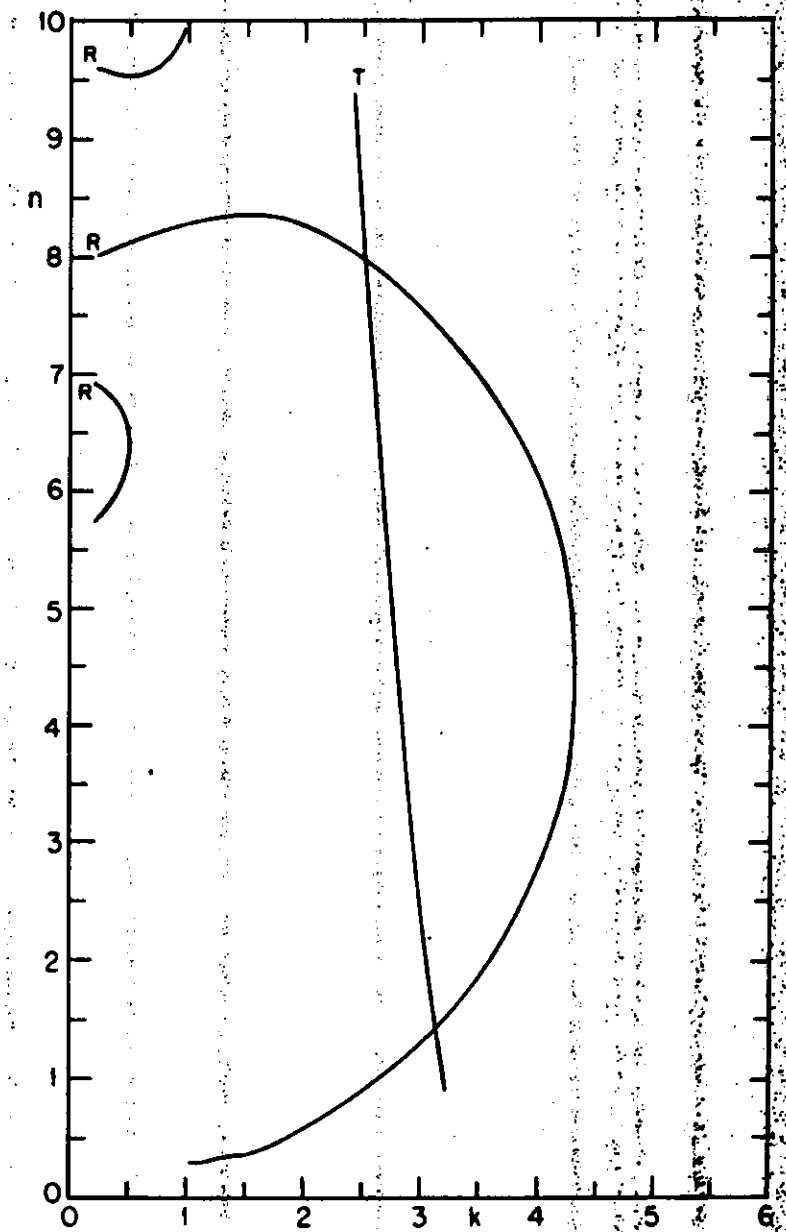

Figure 9a Root-locus diagram of a 500Å Ge Film on a CaF_2 substrate. $\lambda = 2500$Å.

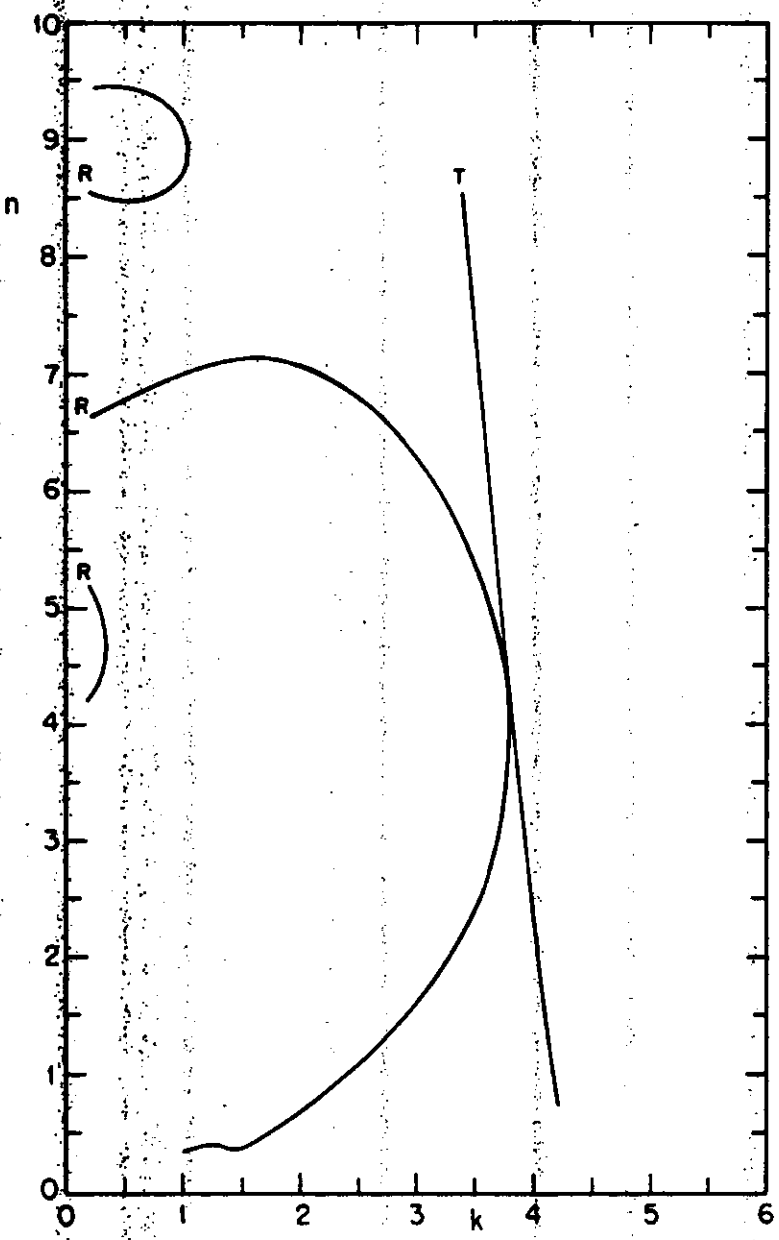

Figure 9b $\lambda = 3000\text{Å}$, $a = 500\text{Å}$.

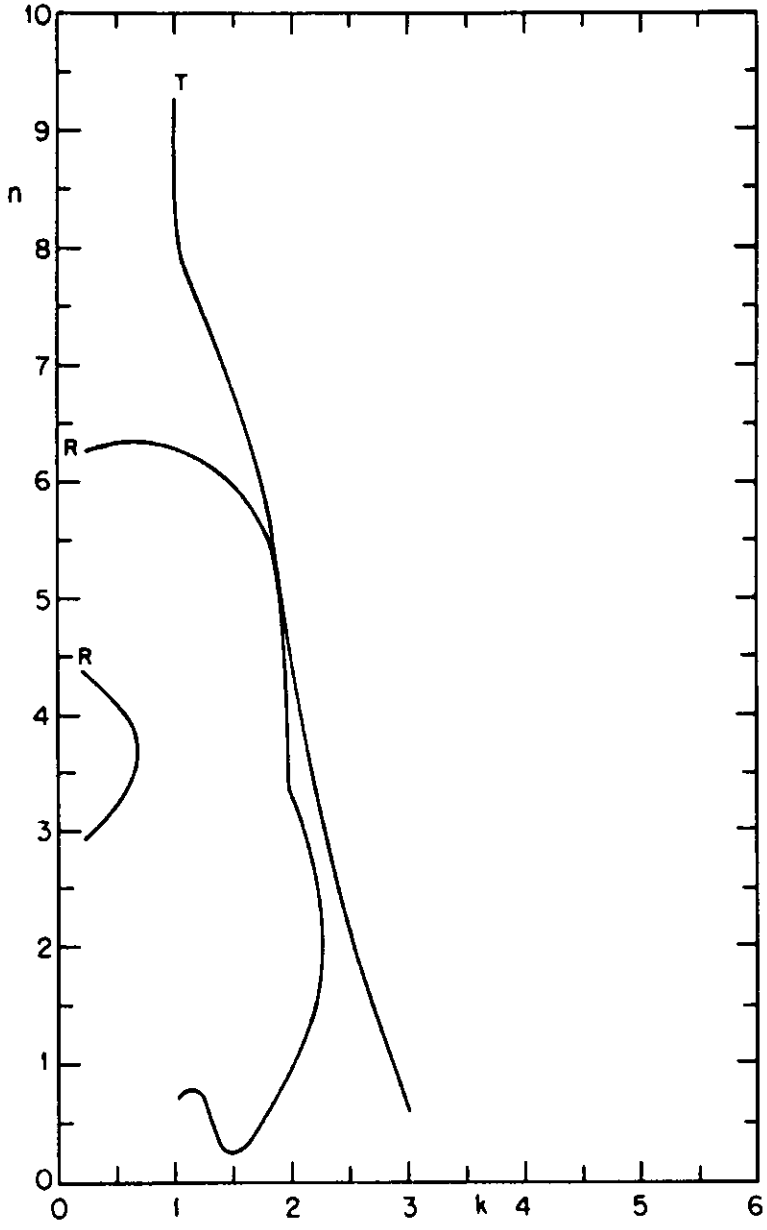

Figure 9c $\lambda = 5500\text{Å}$, $a = 500\text{Å}$.

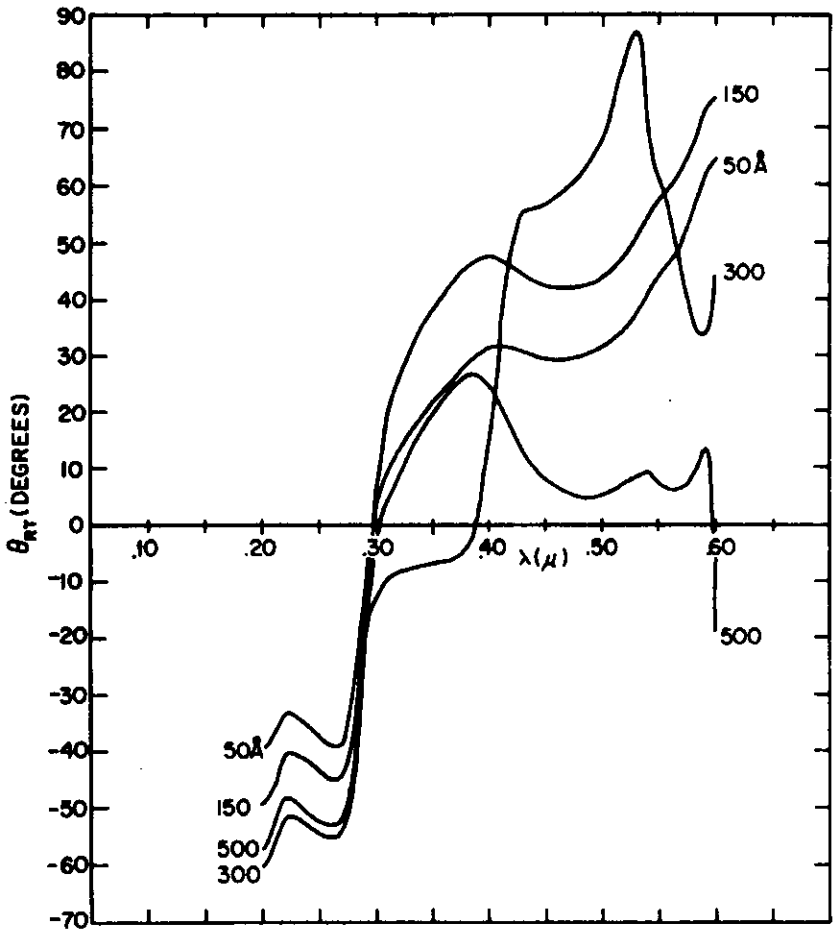

Figure 10 The angle of root-locus intersections, Θ_{RT} vs. λ for the RT model of a Ge film on CaF_2. The film thickness is indicated on each curve.

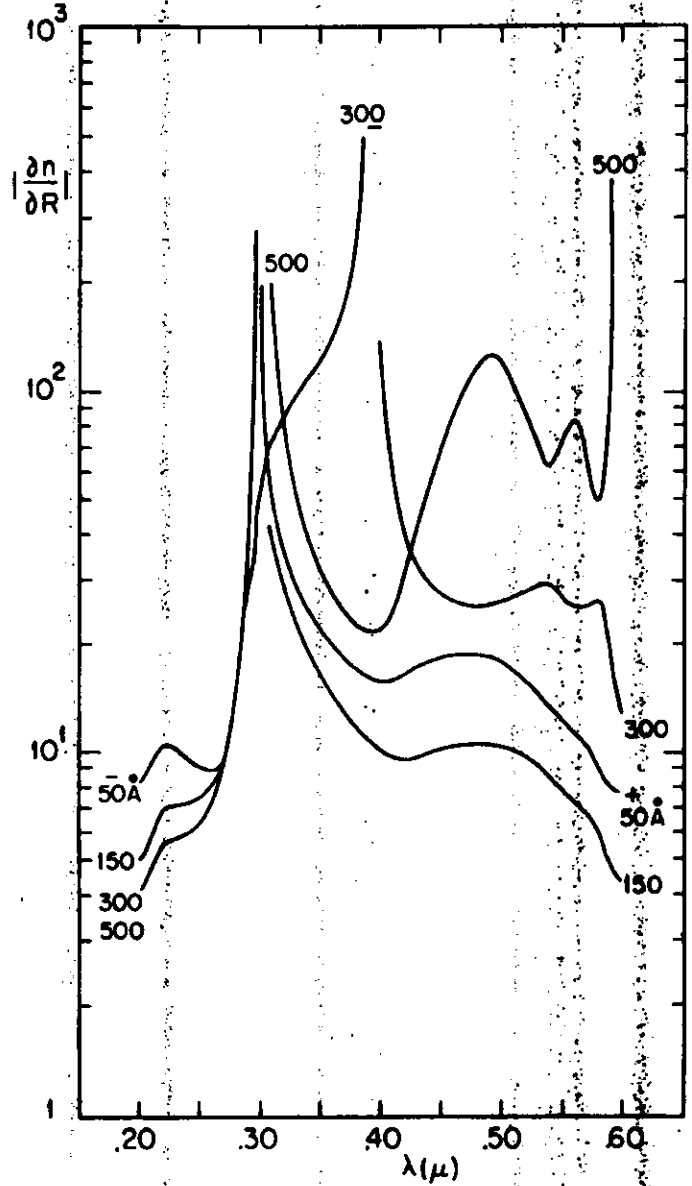

Figure 11a The index of refraction error derivatives vs. λ for the RT model of a Ge film on CaF_2. The sign of the error derivative is indicated for a = 50Å and does not change with thickness unless otherwise noted. $|\partial n/\partial R|$ vs. λ.

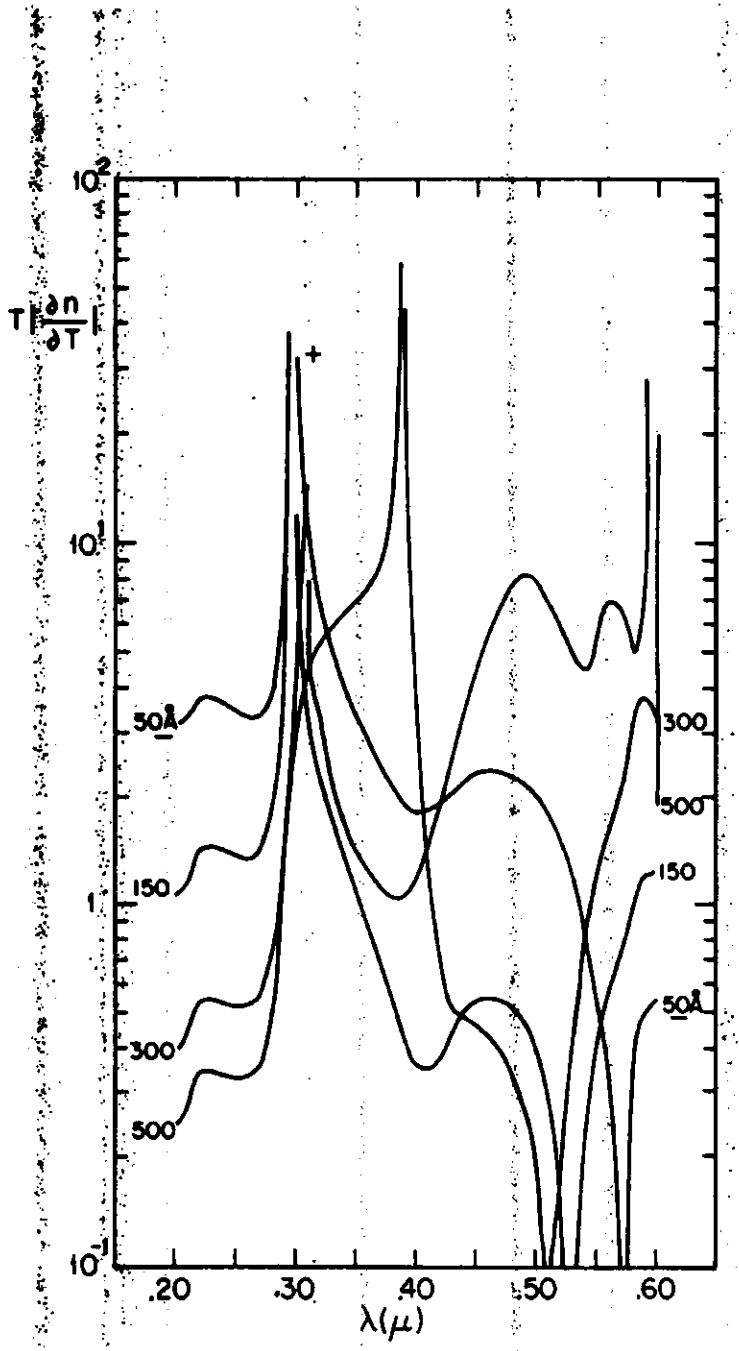

Figure 11b $T|\partial n/\partial T|$ vs. λ

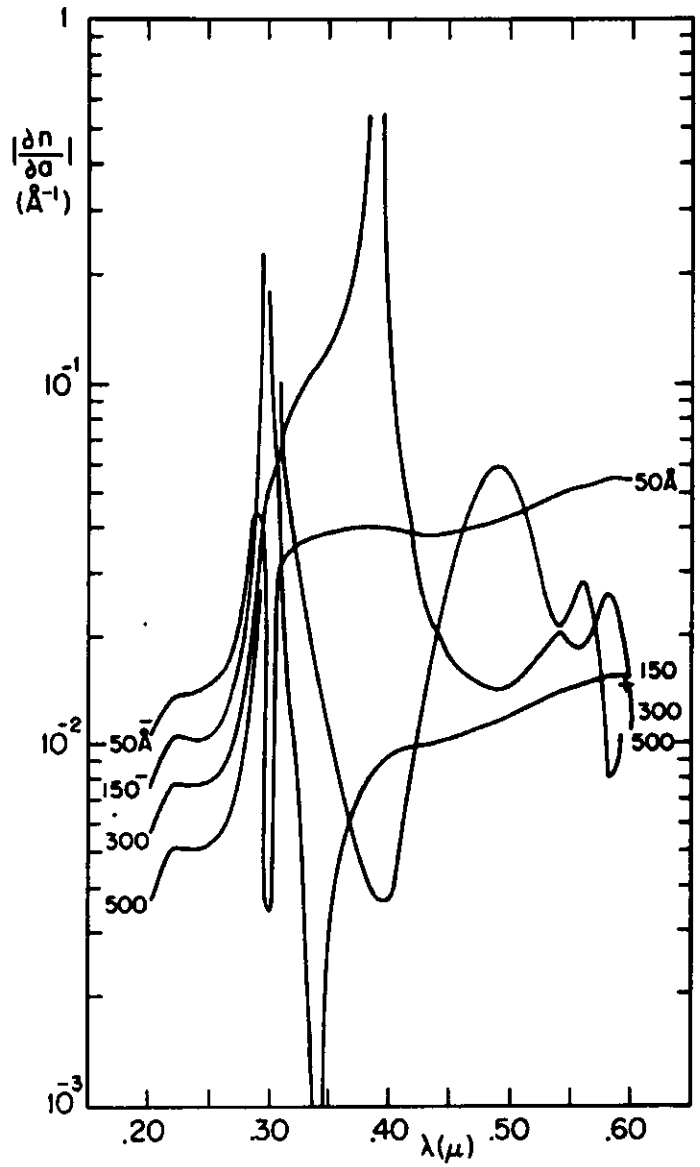

Figure 11c $|\partial n/\partial a|$ vs. λ

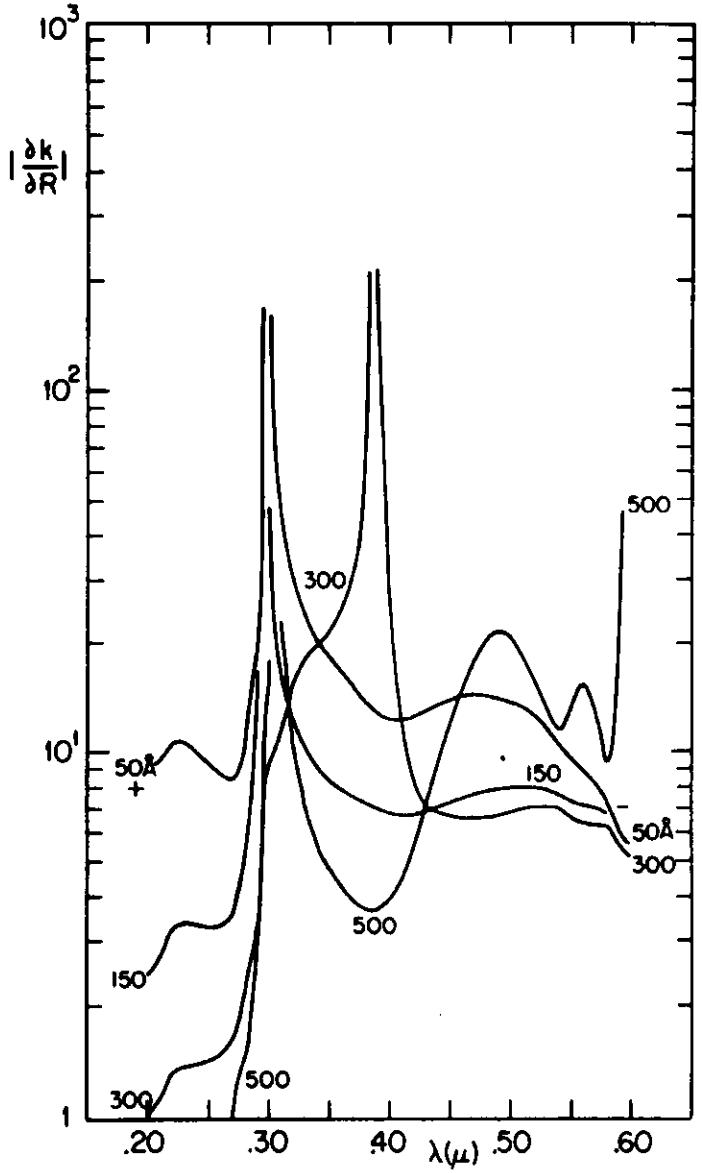

Figure 12a The extinction coefficient error derivatives vs. λ for the RT model. $|\partial k/\partial R|$ vs. λ .

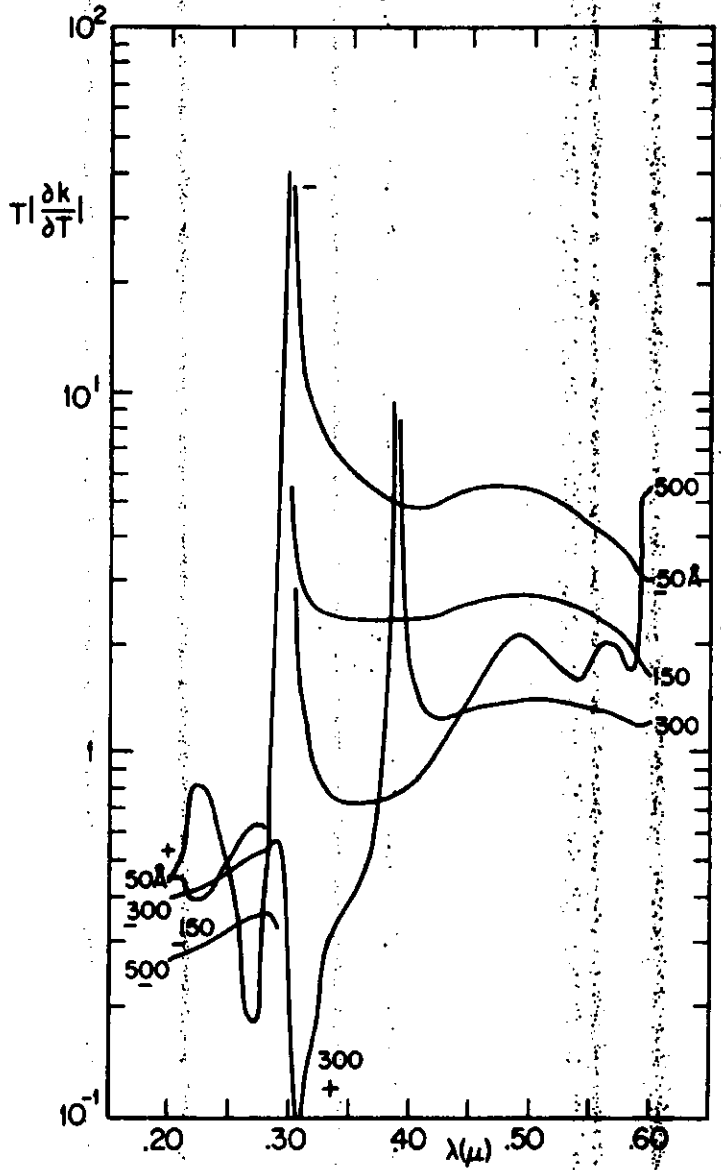

Figure 12b $T|\partial k/\partial T|$ vs. λ .

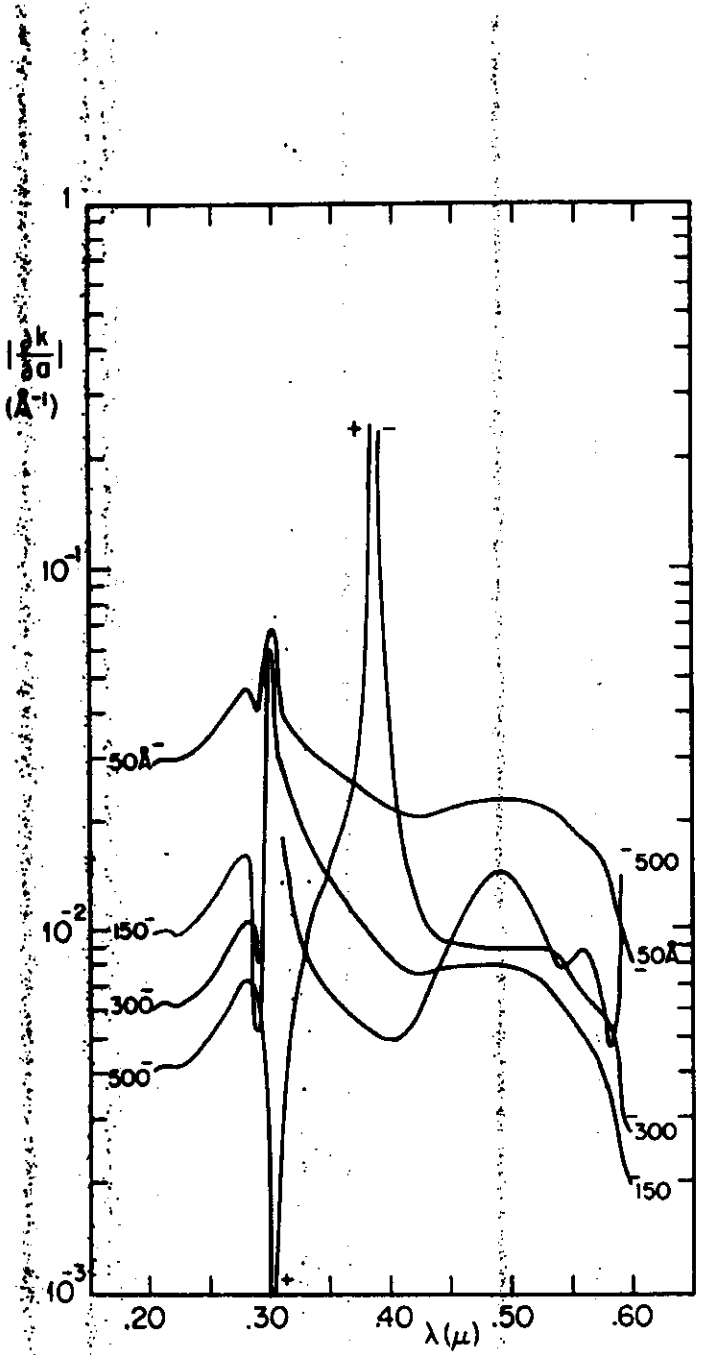

Figure 12c | ∂k/∂α| vs. λ.

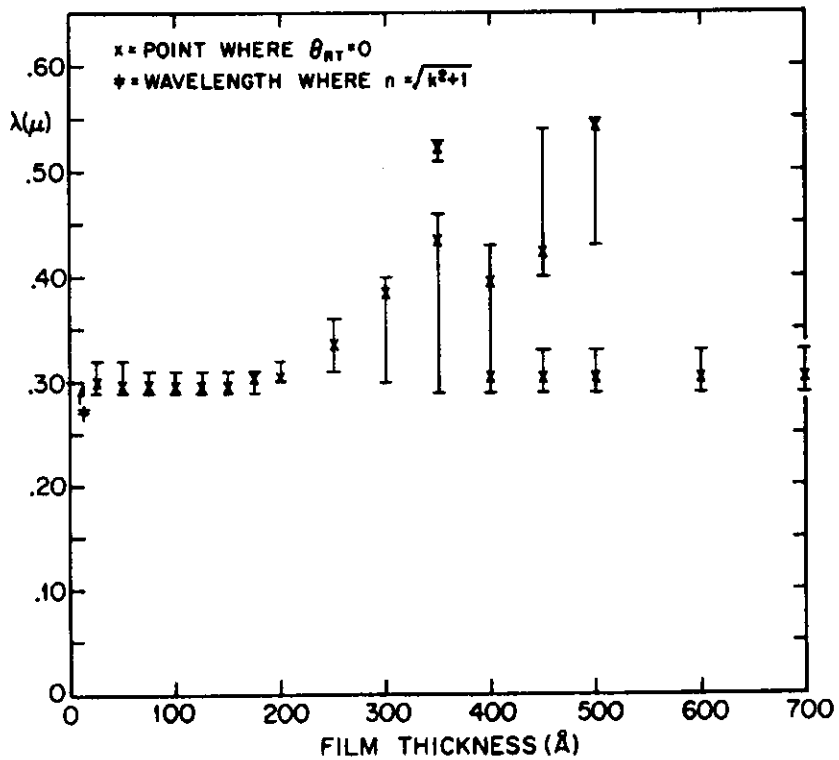

Figure 13 Wavelength region where $|\theta_{RT}| \leq 10^{\circ}$ for the RT model. The limiting value of 10° was chosen arbitrarily as representing an approach to tangency.

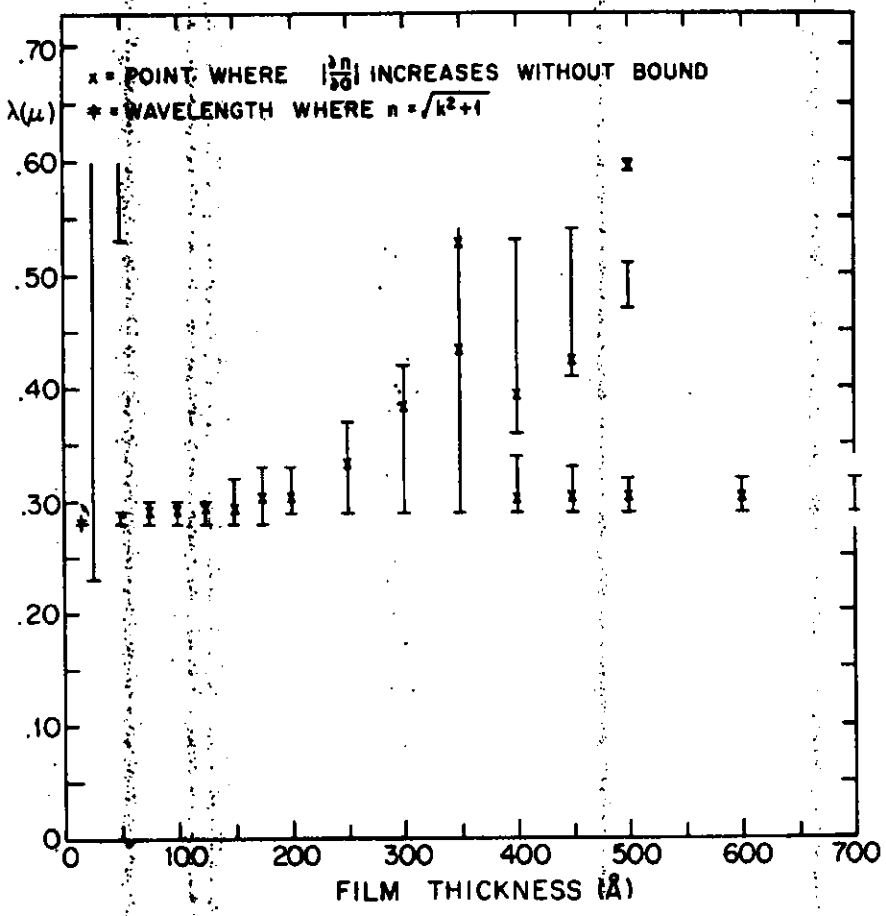

Figure 14c $|\partial n/\partial \alpha| \geq 5 \times 10^{-2}$ Å^{-1}.

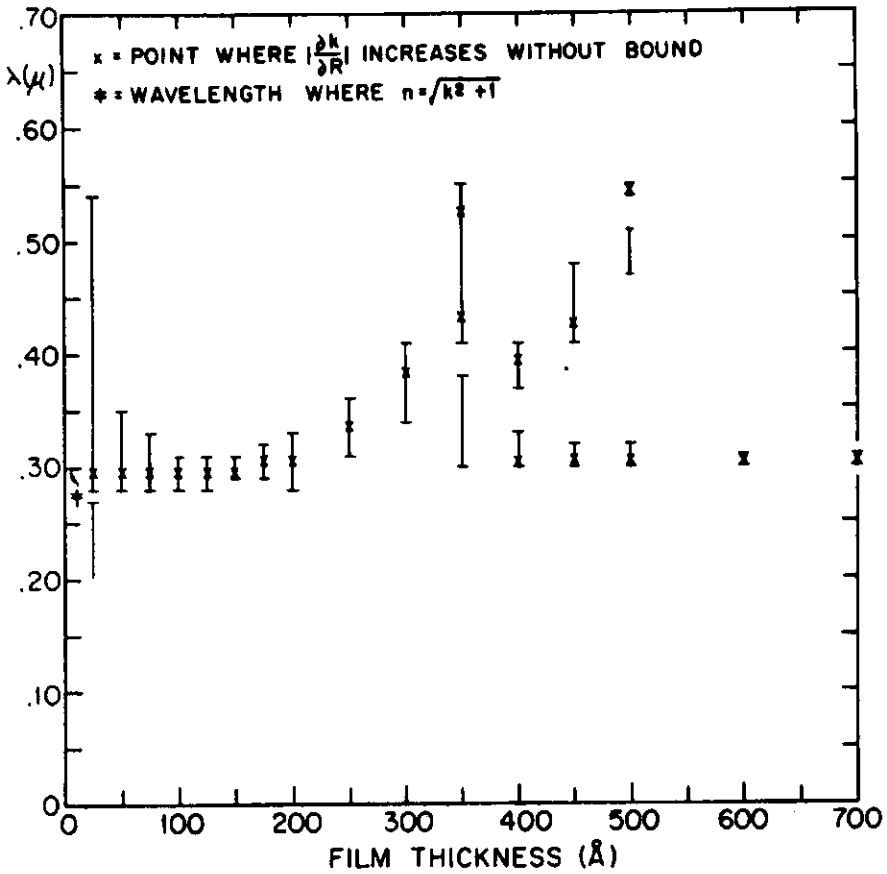

Figure 15a Wavelength region where $|\partial k/\partial R| \geq 20$.

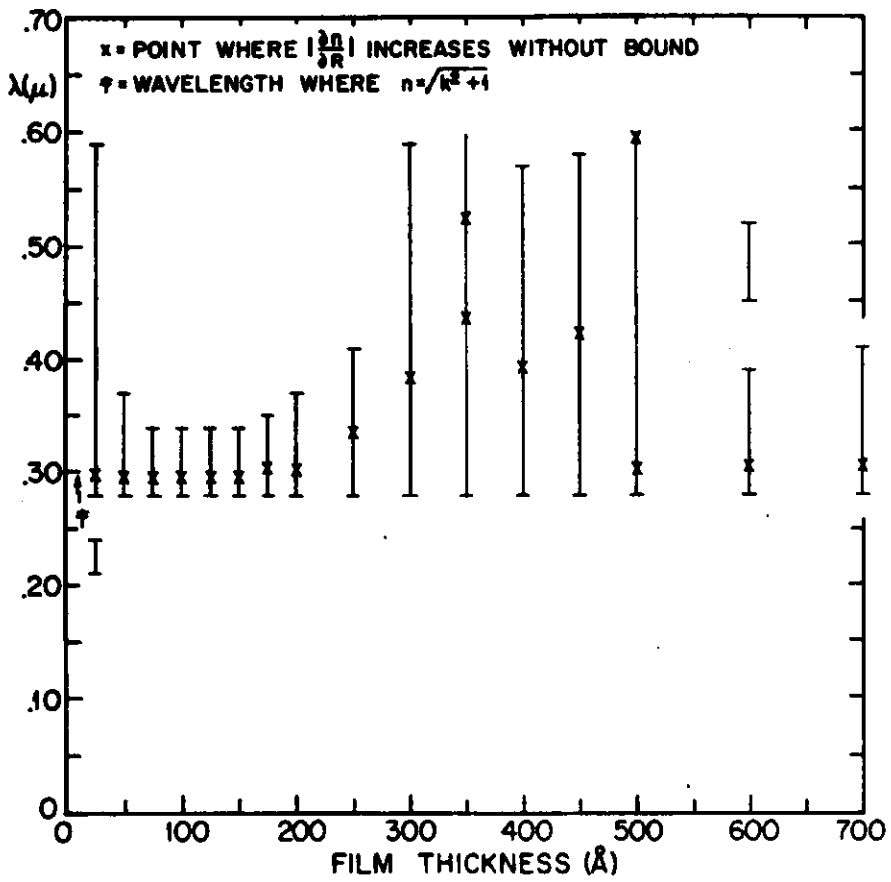

Figure 14a Wavelength region where $|\partial n/\partial R| \geq 20$.

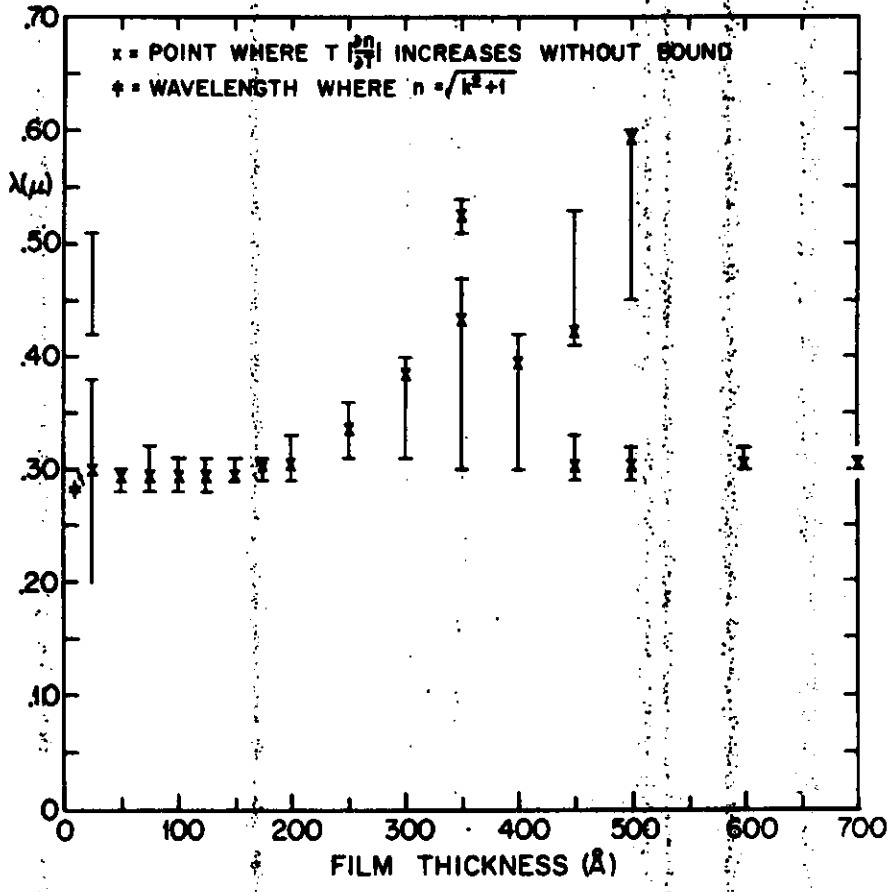

Figure 14b $T|\partial n/\partial T| \geq 5$.

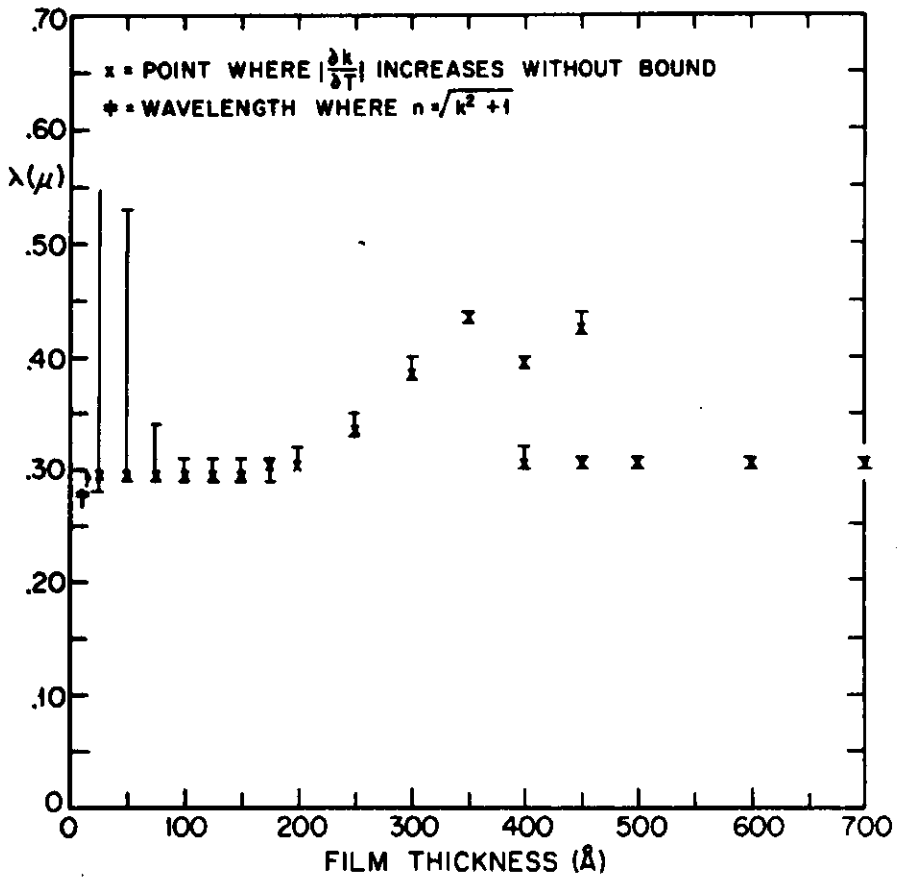

Figure 15b $T\,|\partial k/\partial T| \geq 5$.

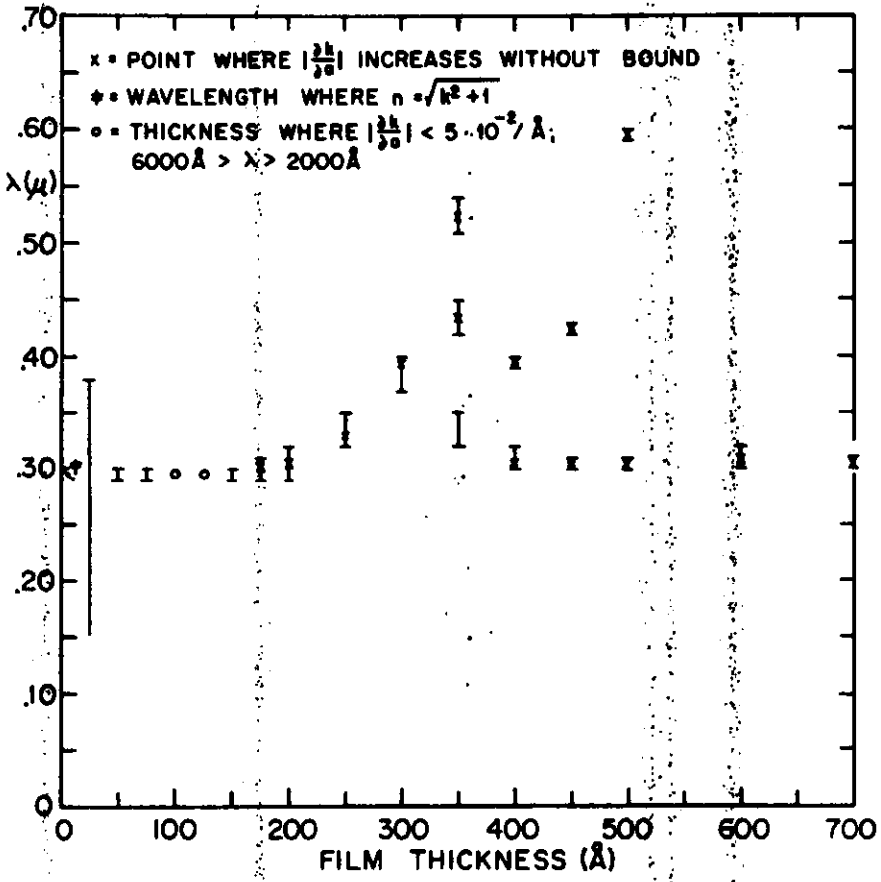

Figure 15c $|\partial k/\partial a| \geq 5 \times 10^{-2}$ Å^{-1}

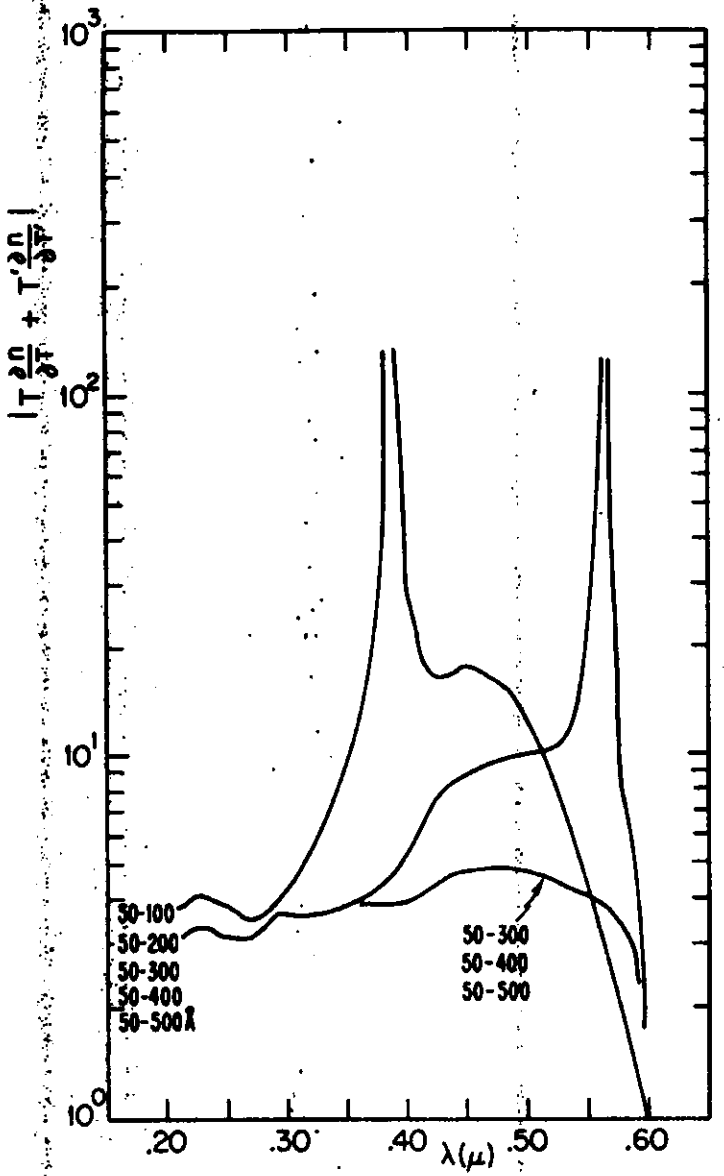

Figure 16a $|T(\partial n/\partial T) + T'(\partial n/\partial T)|$: a' paired with a = 50Å.

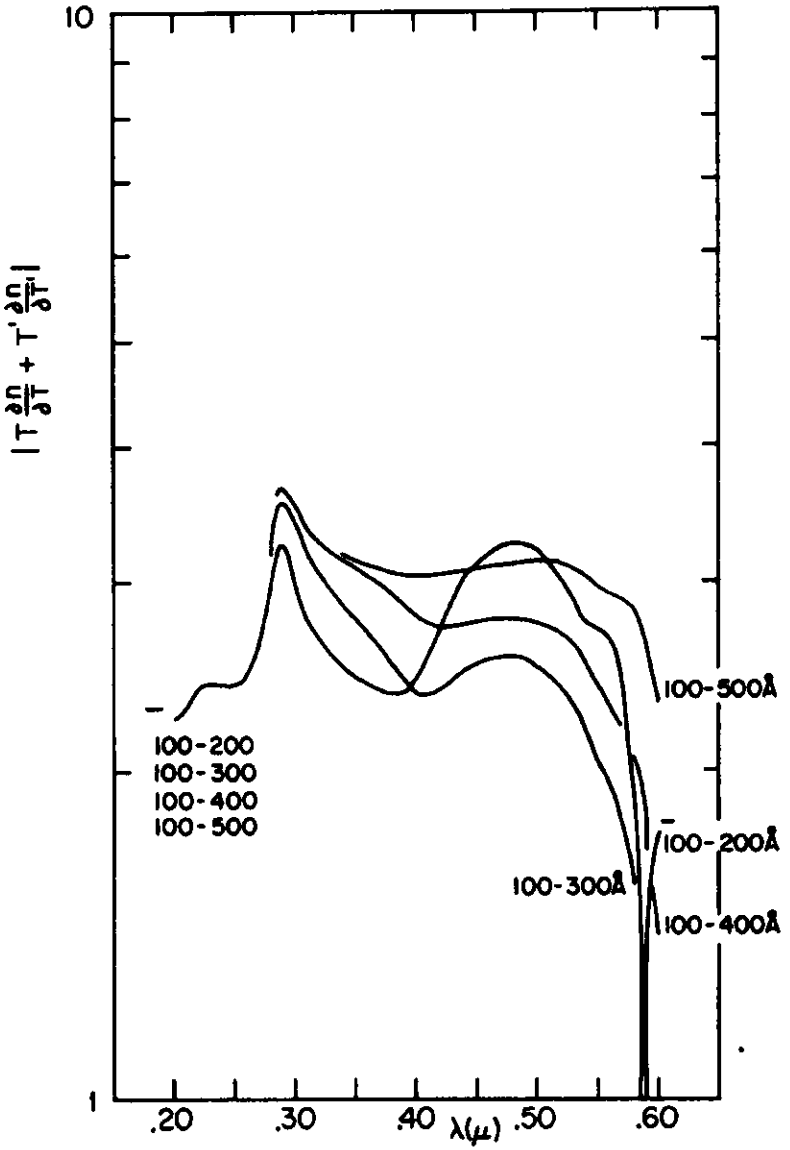

Figure 16b $|T(\partial n/\partial T) + T'(\partial n/\partial T')|$: a' paired with a = 100Å.

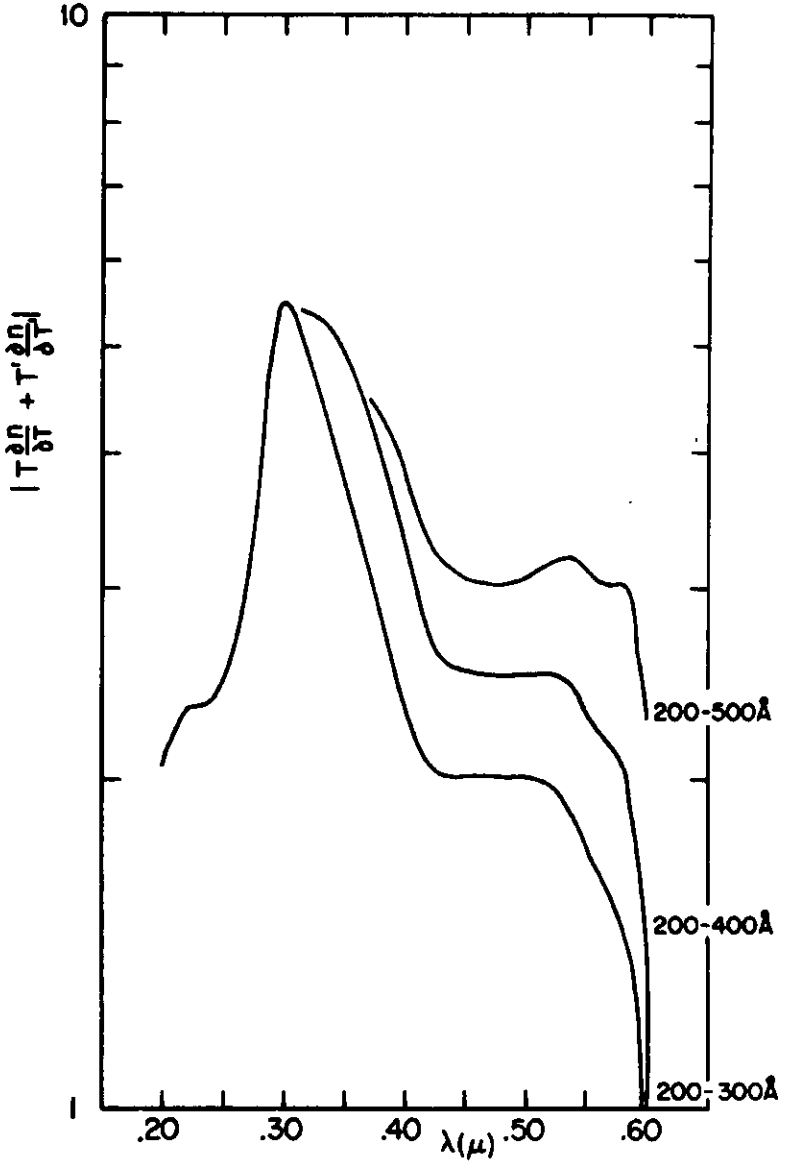

Figure 16c $|T(\partial n/\partial T) + T'(\partial n/\partial T')|$: a' paired with $a = 200$Å.

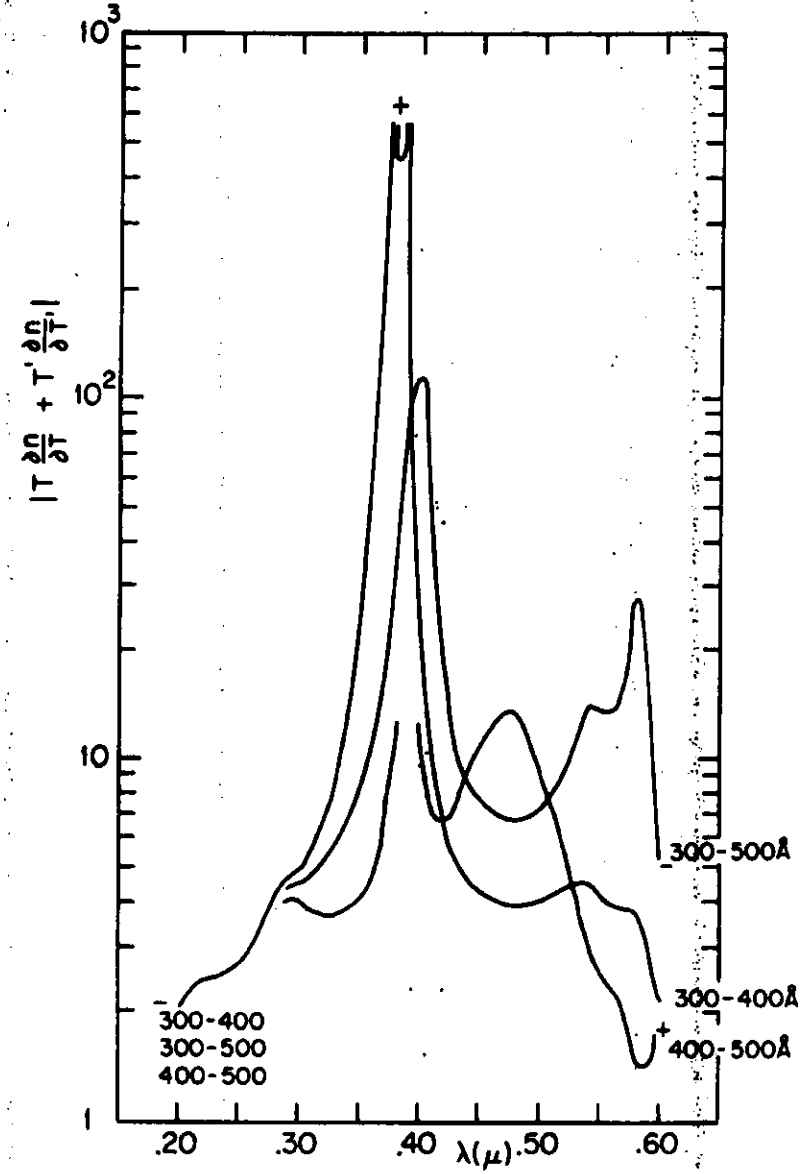

Figure 16d $|T(\partial n/\partial T) + T'(\partial n/\partial T')|$: a' paired with $a = 300$Å and 400Å.

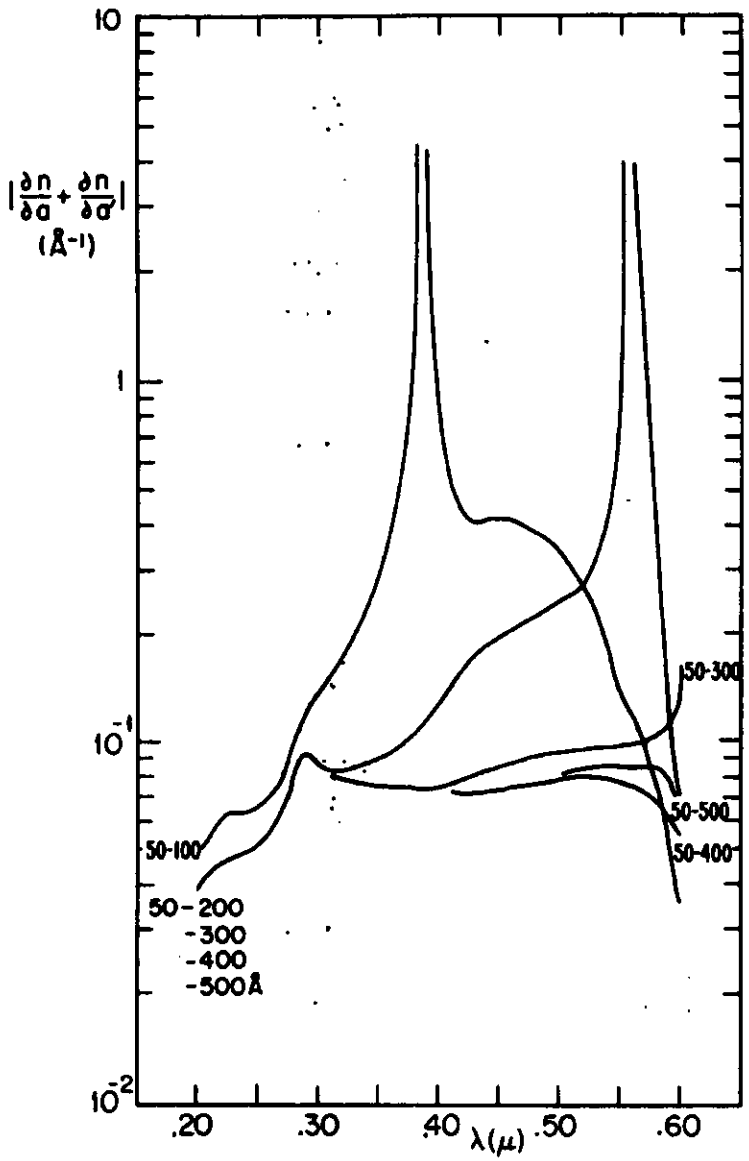

Figure 17a $|(\partial n/\partial a) + (\partial n/\partial a')|$: a' paired with $a = 50Å$.

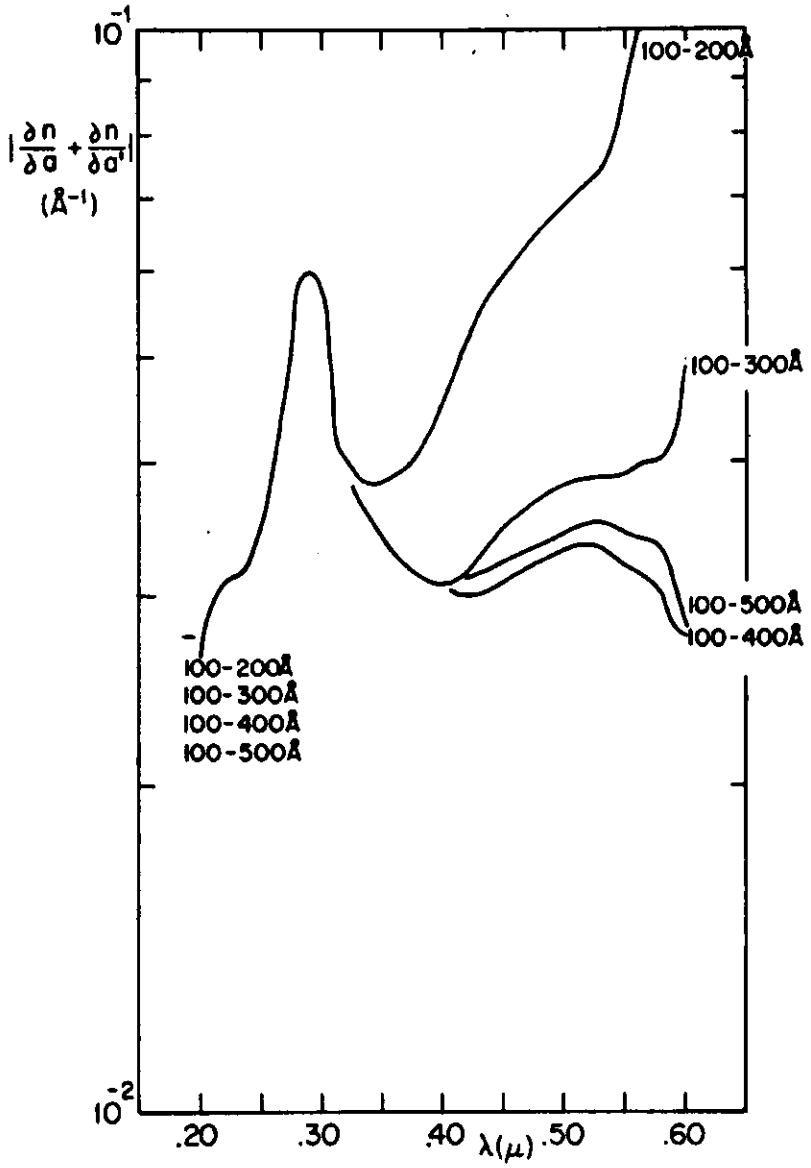

Figure 17b $|(\partial n/\partial a) + (\partial n/\partial a')|$: a' paired with $a = 100Å$.

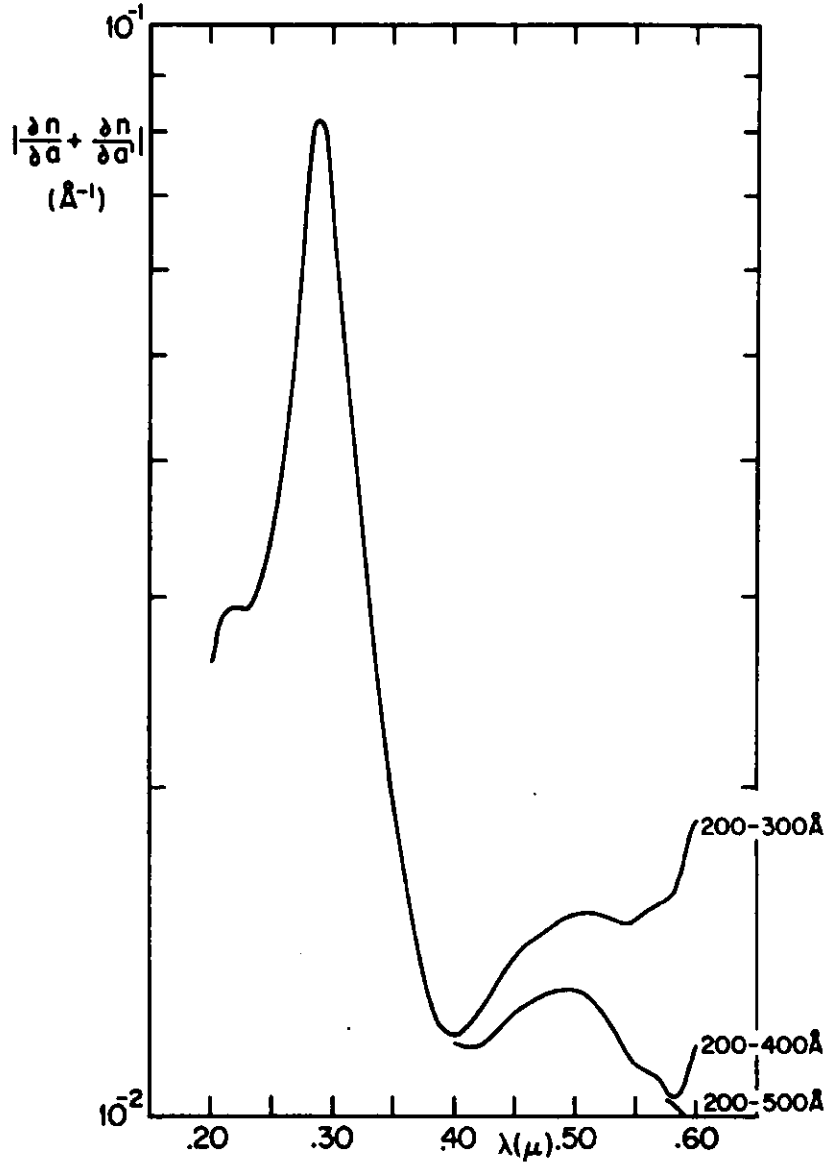

Figure 17c $|(\partial n/\partial a) + (\partial n/\partial a')|$: a' paired with $a = 200Å$.

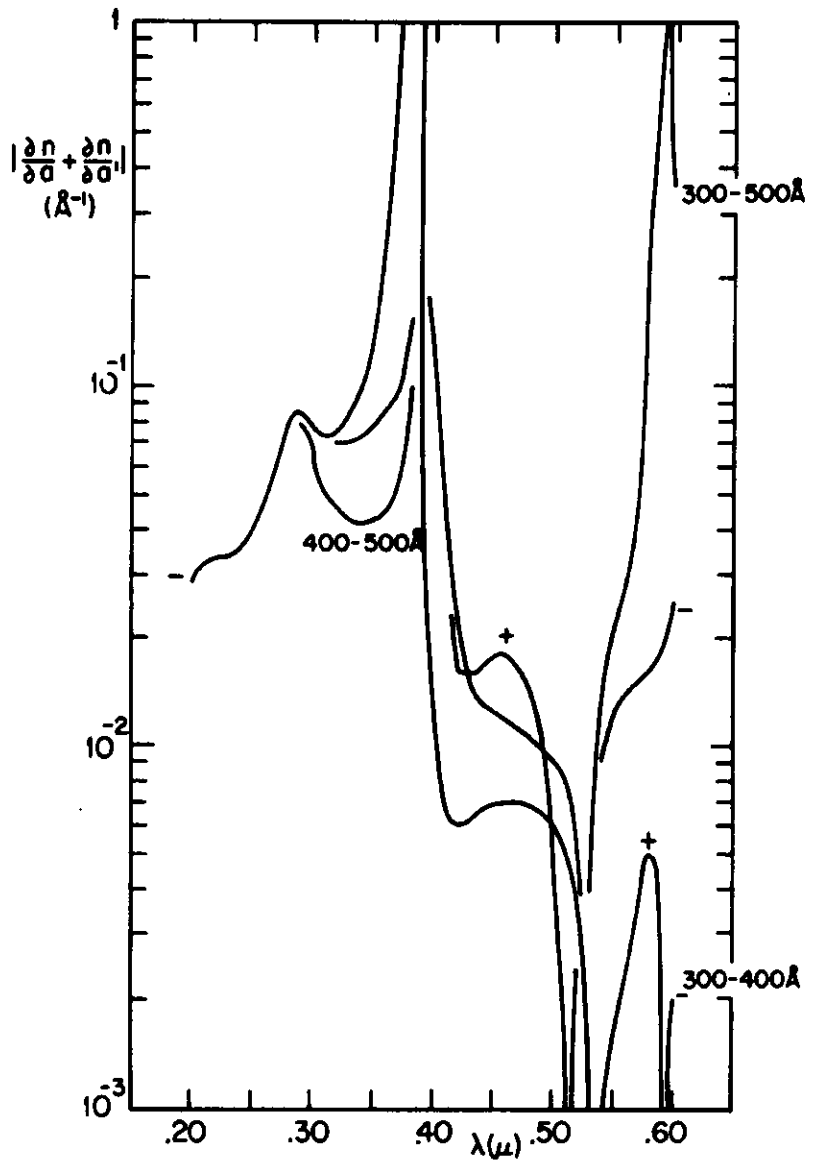

Figure 17d $|(\partial n/\partial a) + (\partial n/\partial a')|$: a' paired with $a = 300Å$ and $400Å$.